Final Report
Ozone Depletion by Bromine and Iodine over the Gulf of Mexico

Prepared for:

Jocelyn Mellberg
Texas Commission on Environmental Quality
12100 Park 35 Circle, MC 164
Austin, TX 78753

Prepared by:

Greg Yarwood, Tanarit Sakulyanontvittaya,
Ou Nopmongcol and Bonyoung Koo
ENVIRON International Corporation
773 San Marin Drive, Suite 2115
Novato, California, 94945
www.environcorp.com
P-415-899-0700
F-415-899-0707

November 2014

ENVIRON

CONTENTS

1.0 INTRODUCTION 1

2.0 CHEMICAL MECHANISM 3

2.1 Base Mechanism: CB6r2 3

2.2 Halogen Chemistry 13

2.2.1 Chlorine Mechanism 13

2.2.2 Bromine Mechanism 16

2.2.3 Iodine 18

2.2.4 Integrated Halogen Mechanism 20

3.0 MODELING DATABASE 24

3.1 "Rider 8" Model for June 2006 24

3.1.1 Halogen emissions from organic sources 27

3.1.2 Halogen emissions from sea-salt 28

3.1.3 Emission Summary 29

3.2 Halogen Boundary Conditions 33

4.0 MODELING RESULTS 34

5.0 CONCLUSIONS AND RECOMMENDATIONS 44

6.0 REFERENCES 46

TABLES

Table 2-1. Reaction listing for CB6r2. 3

Table 2-2. Chemical species included in CB6r2. 12

Table 2-3. Reaction listing for the halogen mechanism. 20

Table 2-4. Chemical species included in CB6r2. 23

Table 3-1. TCEQ 36/12/4 km CAMx nested modeling grids for Rider 8 model of June 2006. 24

Table 3-2. Global annual emissions of halomethanes. 28

Table 3-3. Halogen emissions in the CAMx 12 km grid. 30

Table 3-4. Boundary conditions for halogen species. 33

Table 4-1. Daily ozone depletion (ppb) by halogens at Gulf Coast locations (June 2006 average). 38

Table 4-2. Daily average halogen monoxide (ppt) at receptor locations for June 2006. 39

Table 4-3. Daily average halogen species concentrations (ppt) at Galveston (June 2006 average). 41

Table 4-4. Chemical destruction of Br precursors at Galveston (June 2006 average). 42

FIGURES

Figure 2-1. Relationships between chemical species in the Cl mechanism. 14

Figure 2-2. Relationships between chemical species in the Br mechanism. 17

Figure 2-3. Relationships between chemical species in the I mechanism. 19

Figure 3-1. TCEQ 36/12/4 km CAMx nested modeling grids for the Rider 8 model of June 2006. 25

Figure 3-2. Halogen emissions. 26

Figure 3-3. Example global sea water concentration of chlorophyll-a (mg/m3) from SeaWiFS satellite data. Note that chlorophyll-a also is detected in freshwater lakes. 27

Figure 3-4. Example sea water concentration of chlorophyll-a (mg/m^3) for the CAMx 36 km grid. Note that chlorophyll-a in freshwater lakes has been excluded. 28

Figure 3-5. Spatial distributions of halogen precursor emissions (moles per grid cell per day) for the 12 km grid on June 17 (left) and June 18 (right) for (a) CH_3I, (b) $CHBR_3$, (c) I_2 and (d) SSCL. 31

Figure 3-5. (completed) Spatial distributions of halogen precursor emissions (moles per grid cell per day) for the 12 km grid on June 17 (left) and June 18 (right) for (a) CH_3I, (b) $CHBR_3$, (c) I_2 and (d) SSCL. 32

Figure 4-1. MDA8 ozone on June 17 and 18, 2006 (left and right) without halogen chemistry (CB6r2). 34

Figure 4-2. Differences in MDA8 ozone on June 17 and 18, 2006 (left and right) due to oceanic emissions and reactions of halogens (CB6r2h – CB6r2). 35

Figure 4-3. Differences in MDA8 ozone on June 17 and 18, 2006 (left and right) due to reactions of Bromine, Iodine and Chlorine (note: scale maxima differ by row). 36

Figure 4-4. Monthly maximum and average (left and right) concentrations of BrO, IO and ClO (note: scale maxima differ by figure). 37

Figure 4-5. Hourly profiles of ozone depletion by halogens at Galveston (left) and Conroe (right) (June 2006 average). 38

Figure 4-6. Hourly profile of Cl species concentrations (ppt) at Galveston (June 2006 average). 40

Figure 4-7. Hourly profile of Br species concentrations (ppt) at Galveston (June 2006 average). 42

Figure 4-8. Hourly profile of I species concentrations (ppt) at Galveston (June 2006 average). 43

1.0 INTRODUCTION

The Texas Commission on Environmental Quality (TCEQ) is responsible for developing the Texas State Implementation Plan (SIP) to demonstrate compliance with the National Ambient Air Quality Standard (NAAQS) for ozone in Texas. Currently, the ozone NAAQS is set at 75 parts per billion (ppb) for the three year running average of the annual fourth highest daily maximum 8-hour average (MDA8) at each monitoring location. Under the Clean Air Act, the Environmental Protection Agency (EPA) is required to review the NAAQS periodically. EPA's next review of the ozone standard is scheduled to be completed in late 2014. Throughout the Obama Administration, the EPA has suggested that it will consider setting a revised standard in the range 60-70 ppb. The ozone concentration in background air entering Texas may be as low as 10 ppb for clean air from the Gulf of Mexico or may approach the level of the NAAQS for air of continental origin that has been modified by input of anthropogenic emissions. Correctly characterizing background ozone is very important to SIP planning because over-estimating background may lead to implementation of emission control strategies that are more costly than needed to protect public health.

The TCEQ uses the Comprehensive Air Quality Model with Extensions (CAMx) for ozone SIP modeling. CAMx ozone predictions for Gulf Coast monitors are frequently biased high when air flow is from the Gulf. CAMx ozone predictions for Gulf Coast monitors depend upon emissions and chemistry over the Gulf and the CAMx boundary conditions (BCs) for the Gulf and southern Atlantic Ocean which describe ozone concentrations entering CAMx and arriving in the Gulf. The TCEQ obtains CAMx BCs from a global model, GEOS-Chem, which tends to over predict ozone in the Gulf as do many other global models (Yarwood et al., 2012). It appears that regional and global models consistently over predict ozone in the Gulf of Mexico during the ozone season.

Previously, CAMx was extended to model ozone depletion by iodine compounds emitted from ocean waters such as the Gulf of Mexico (Yarwood et al., 2012). Iodine can cause ozone depletion of several parts ppb per day within the marine boundary layer (Mahajan et al., 2010 and references therein). The development of the CAMx iodine chemistry made use of field study data from the Cape Verde Islands (in the Atlantic; 17 N, 25 W) which show that bromine chemistry operates in synergy with iodine chemistry to double the rate of ozone depletion in the marine boundary layer (Mahajan et al., 2010). This purpose of this project was to add bromine chemistry to the iodine chemistry developed for CAMx and quantify the impact on modeled background ozone over the Gulf. Emissions of inorganic iodine compounds (I_2 and HOI) are caused by deposition of ozone (O_3) to ocean waters (Carpenter et al., 2013) whereas emissions of organic iodine and bromine compounds result from biological processes (Carpenter, 2003). Sea-salt aerosol produced by bubble bursting and wind shear at the ocean surface is the dominant source of inorganic bromine and chlorine input to marine air (Sander et al., 2003).

A consistent halogen mechanism for chlorine, bromine and iodine was developed and integrated with the CB6r2 ozone chemistry mechanism used by the TCEQ as described in Section 2 of this report. The combine mechanism may be referred to as CB6r2h. Halogen emissions from the Gulf were estimated as described in Section 3. The results of CAMx

simulations with CB6r2h are presented and discussed in Section 4 and conclusions and recommendations are presented in Section 5.

2.0 CHEMICAL MECHANISM

We developed a chemical mechanism for bromine that is compatible with the latest version of the Carbon Bond chemical mechanism implemented in CAMx, namely revision 2 of Carbon Bond 6 (CB6r2). The bromine reactions were integrated with previously developed reactions for iodine (Yarwood et al., 2012) and chlorine (Tanaka et al., 2003a; Koo et al., 2012) with rate constants updated to currently accepted values (IUPAC, 2014a and b) and mechanism revisions to promote consistency.

2.1 Base Mechanism: CB6r2

The chemical reactions in the CB6r2 mechanism are listed in Table 2-1 and the chemical species names are defined in Table 2-2. CB6r2 has 216 chemical reactions and 80 chemical species of which 5 (M, O2, H2O H2 and CH4) are set by CAMx rather than determined by emissions. CH4 represents background methane and is set to 1.75 ppm by CAMx. The species ECH4 may be used to model the effect of emitted methane on top of the background methane represented by CH4.

Table 2-1. Reaction listing for CB6r2.

No.	Reactants and Products	Rate Constant Expression	k_{298}
1	NO2 = NO + O	Photolysis	6.30E-3
2	O + O2 + M = O3 + M	k = 5.68E-34 (T/300)^-2.6	5.78E-34
3	O3 + NO = NO2	k = 1.40E-12 exp(-1310/T)	1.73E-14
4	O + NO + M = NO2 + M	k = 1.00E-31 (T/300)^-1.6	1.01E-31
5	O + NO2 = NO	k = 5.50E-12 exp(188/T)	1.03E-11
6	O + NO2 = NO3	Falloff: F=0.6; n=1 k(0) = 1.30E-31 (T/300)^-1.5 k(inf) = 2.30E-11 (T/300)^0.24	2.11E-12
7	O + O3 =	k = 8.00E-12 exp(-2060/T)	7.96E-15
8	O3 = O	Photolysis	3.33E-4
9	O3 = O1D	Photolysis	8.78E-6
10	O1D + M = O + M	k = 2.23E-11 exp(115/T)	3.28E-11
11	O1D + H2O = 2 OH	k = 2.14E-10	2.14E-10
12	O3 + OH = HO2	k = 1.70E-12 exp(-940/T)	7.25E-14
13	O3 + HO2 = OH	k = 2.03E-16 (T/300)^4.57 exp(693/T)	2.01E-15
14	OH + O = HO2	k = 2.40E-11 exp(110/T)	3.47E-11
15	HO2 + O = OH	k = 2.70E-11 exp(224/T)	5.73E-11
16	OH + OH = O	k = 6.20E-14 (T/298)^2.6 exp(945/T)	1.48E-12
17	OH + OH = H2O2	Falloff: F=0.5; n=1.13 k(0) = 6.90E-31 (T/300)^-0.8 k(inf) = 2.60E-11	5.25E-12
18	OH + HO2 =	k = 4.80E-11 exp(250/T)	1.11E-10
19	HO2 + HO2 = H2O2	k = k1 + k2 [M] k1 = 2.20E-13 exp(600/T) k2 = 1.90E-33 exp(980/T)	2.90E-12
20	HO2 + HO2 + H2O = H2O2	k = k1 + k2 [M] k1 = 3.08E-34 exp(2800/T) k2 = 2.66E-54 exp(3180/T)	6.53E-30
21	H2O2 = 2 OH	Photolysis	3.78E-6

No.	Reactants and Products	Rate Constant Expression	k_{298}
22	H2O2 + OH = HO2	k = 2.90E-12 exp(-160/T)	1.70E-12
23	H2O2 + O = OH + HO2	k = 1.40E-12 exp(-2000/T)	1.70E-15
24	NO + NO + O2 = 2 NO2	k = 3.30E-39 exp(530/T)	1.95E-38
25	HO2 + NO = OH + NO2	k = 3.45E-12 exp(270/T)	8.54E-12
26	NO2 + O3 = NO3	k = 1.40E-13 exp(-2470/T)	3.52E-17
27	NO3 = NO2 + O	Photolysis	1.56E-1
28	NO3 = NO	Photolysis	1.98E-2
29	NO3 + NO = 2 NO2	k = 1.80E-11 exp(110/T)	2.60E-11
30	NO3 + NO2 = NO + NO2	k = 4.50E-14 exp(-1260/T)	6.56E-16
31	NO3 + O = NO2	k = 1.70E-11	1.70E-11
32	NO3 + OH = HO2 + NO2	k = 2.00E-11	2.00E-11
33	NO3 + HO2 = OH + NO2	k = 4.00E-12	4.00E-12
34	NO3 + O3 = NO2	k = 1.00E-17	1.00E-17
35	NO3 + NO3 = 2 NO2	k = 8.50E-13 exp(-2450/T)	2.28E-16
36	NO3 + NO2 = N2O5	Falloff: F=0.35; n=1.33 k(0) = 3.60E-30 (T/300)^-4.1 k(inf) = 1.90E-12 (T/300)^0.2	1.24E-12
37	N2O5 = NO3 + NO2	Falloff: F=0.35; n=1.33 k(0) = 1.30E-3 (T/300)^-3.5 exp(-11000/T) k(inf) = 9.70E+14 (T/300)^0.1 exp(-11080/T)	4.46E-2
38	N2O5 = NO2 + NO3	Photolysis	2.52E-5
39	N2O5 + H2O = 2 HNO3	k = 1.00E-22	1.00E-22
40	NO + OH = HONO	Falloff: F=0.81; n=0.87 k(0) = 7.40E-31 (T/300)^-2.4 k(inf) = 3.30E-11 (T/300)^-0.3	9.77E-12
41	NO + NO2 + H2O = 2 HONO	k = 5.00E-40	5.00E-40
42	HONO + HONO = NO + NO2	k = 1.00E-20	1.00E-20
43	HONO = NO + OH	Photolysis	1.04E-3
44	HONO + OH = NO2	k = 2.50E-12 exp(260/T)	5.98E-12
45	NO2 + OH = HNO3	Falloff: F=0.6; n=1 k(0) = 1.80E-30 (T/300)^-3 k(inf) = 2.80E-11	1.06E-11
46	HNO3 + OH = NO3	k = k1 + k3 [M] / (1 + k3 [M] / k2) k1 = 2.40E-14 exp(460/T) k2 = 2.70E-17 exp(2199/T) k3 = 6.50E-34 exp(1335/T)	1.54E-13
47	HNO3 = OH + NO2	Photolysis	2.54E-7
48	HO2 + NO2 = PNA	Falloff: F=0.6; n=1 k(0) = 1.80E-31 (T/300)^-3.2 k(inf) = 4.70E-12	1.38E-12
49	PNA = HO2 + NO2	Falloff: F=0.6; n=1 k(0) = 4.10E-5 exp(-10650/T) k(inf) = 4.80E+15 exp(-11170/T)	8.31E-2
50	PNA = 0.59 HO2 + 0.59 NO2 + 0.41 OH + 0.41 NO3	Photolysis	2.36E-6
51	PNA + OH = NO2	k = 3.20E-13 exp(690/T)	3.24E-12
52	SO2 + OH = SULF + HO2	Falloff: F=0.53; n=1.1 k(0) = 4.50E-31 (T/300)^-3.9 k(inf) = 1.30E-12 (T/300)^-0.7	8.12E-13
53	C2O3 + NO = NO2 + MEO2 + RO2	k = 7.50E-12 exp(290/T)	1.98E-11

No.	Reactants and Products	Rate Constant Expression	k_{298}
54	C2O3 + NO2 = PAN	Falloff: F=0.3; n=1.41 k(0) = 2.70E-28 (T/300)^-7.1 k(inf) = 1.20E-11 (T/300)^-0.9	9.40E-12
55	PAN = NO2 + C2O3	Falloff: F=0.3; n=1.41 k(0) = 4.90E-3 exp(-12100/T) k(inf) = 5.40E+16 exp(-13830/T)	2.98E-4
56	PAN = 0.6 NO2 + 0.6 C2O3 + 0.4 NO3 + 0.4 MEO2 + 0.4 RO2	Photolysis	3.47E-7
57	C2O3 + HO2 = 0.41 PACD + 0.15 AACD + 0.15 O3 + 0.44 MEO2 + 0.44 RO2 + 0.44 OH	k = 5.20E-13 exp(980/T)	1.39E-11
58	C2O3 + RO2 = C2O3	k = 8.90E-13 exp(800/T)	1.30E-11
59	C2O3 + C2O3 = 2 MEO2 + 2 RO2	k = 2.90E-12 exp(500/T)	1.55E-11
60	C2O3 + CXO3 = MEO2 + ALD2 + XO2H + 2 RO2	k = 2.90E-12 exp(500/T)	1.55E-11
61	CXO3 + NO = NO2 + ALD2 + XO2H + RO2	k = 6.70E-12 exp(340/T)	2.10E-11
62	CXO3 + NO2 = PANX	k = k(ref) K k(ref) = k(54) K = 1.00E+0	9.40E-12
63	PANX = NO2 + CXO3	k = k(ref) K k(ref) = k(55) K = 1.00E+0	2.98E-4
64	PANX = 0.6 NO2 + 0.6 CXO3 + 0.4 NO3 + 0.4 ALD2 + 0.4 XO2H + 0.4 RO2	Photolysis	3.47E-7
65	CXO3 + HO2 = 0.41 PACD + 0.15 AACD + 0.15 O3 + 0.44 ALD2 + 0.44 XO2H + 0.44 RO2 + 0.44 OH	k = 5.20E-13 exp(980/T)	1.39E-11
66	CXO3 + RO2 = 0.8 ALD2 + 0.8 XO2H + 0.8 RO2	k = 8.90E-13 exp(800/T)	1.30E-11
67	CXO3 + CXO3 = 2 ALD2 + 2 XO2H + 2 RO2	k = 3.20E-12 exp(500/T)	1.71E-11
68	RO2 + NO = NO	k = 2.40E-12 exp(360/T)	8.03E-12
69	RO2 + HO2 = HO2	k = 4.80E-13 exp(800/T)	7.03E-12
70	RO2 + RO2 =	k = 6.50E-14 exp(500/T)	3.48E-13
71	MEO2 + NO = FORM + HO2 + NO2	k = 2.30E-12 exp(360/T)	7.70E-12
72	MEO2 + HO2 = 0.9 MEPX + 0.1 FORM	k = 3.80E-13 exp(780/T)	5.21E-12
73	MEO2 + C2O3 = FORM + 0.9 HO2 + 0.9 MEO2 + 0.1 AACD + 0.9 RO2	k = 2.00E-12 exp(500/T)	1.07E-11
74	MEO2 + RO2 = 0.685 FORM + 0.315 MEOH + 0.37 HO2 + RO2	k = k(ref) K k(ref) = k(70) K = 1.00E+0	3.48E-13
75	XO2H + NO = NO2 + HO2	k = 2.70E-12 exp(360/T)	9.04E-12
76	XO2H + HO2 = ROOH	k = 6.80E-13 exp(800/T)	9.96E-12
77	XO2H + C2O3 = 0.8 HO2 + 0.8 MEO2 + 0.2 AACD + 0.8 RO2	k = k(ref) K k(ref) = k(58) K = 1.00E+0	1.30E-11
78	XO2H + RO2 = 0.6 HO2 + RO2	k = k(ref) K k(ref) = k(70) K = 1.00E+0	3.48E-13
79	XO2 + NO = NO2	k = k(ref) K k(ref) = k(75) K = 1.00E+0	9.04E-12
80	XO2 + HO2 = ROOH	k = k(ref) K k(ref) = k(76) K = 1.00E+0	9.96E-12

No.	Reactants and Products	Rate Constant Expression	k_{298}
81	XO2 + C2O3 = 0.8 MEO2 + 0.2 AACD + 0.8 RO2	k = k(ref) K k(ref) = k(58) K = 1.00E+0	1.30E-11
82	XO2 + RO2 = RO2	k = k(ref) K k(ref) = k(70) K = 1.00E+0	3.48E-13
83	XO2N + NO = 0.5 NTR1 + 0.5 NTR2	k = k(ref) K k(ref) = k(75) K = 1.00E+0	9.04E-12
84	XO2N + HO2 = ROOH	k = k(ref) K k(ref) = k(76) K = 1.00E+0	9.96E-12
85	XO2N + C2O3 = 0.8 HO2 + 0.8 MEO2 + 0.2 AACD + 0.8 RO2	k = k(ref) K k(ref) = k(58) K = 1.00E+0	1.30E-11
86	XO2N + RO2 = RO2	k = k(ref) K k(ref) = k(70) K = 1.00E+0	3.48E-13
87	MEPX + OH = 0.6 MEO2 + 0.6 RO2 + 0.4 FORM + 0.4 OH	k = 5.30E-12 exp(190/T)	1.00E-11
88	MEPX = MEO2 + RO2 + OH	Photolysis	2.68E-6
89	ROOH + OH = 0.54 XO2H + 0.06 XO2N + 0.6 RO2 + 0.4 OH	k = 5.30E-12 exp(190/T)	1.00E-11
90	ROOH = HO2 + OH	Photolysis	2.68E-6
91	NTR1 + OH = NTR2	k = 2.00E-12	2.00E-12
92	NTR1 = NO2	Photolysis	1.06E-6
93	FACD + OH = HO2	k = 4.50E-13	4.50E-13
94	AACD + OH = MEO2 + RO2	k = 4.00E-14 exp(850/T)	6.93E-13
95	PACD + OH = C2O3	k = 5.30E-12 exp(190/T)	1.00E-11
96	FORM + OH = HO2 + CO	k = 5.40E-12 exp(135/T)	8.49E-12
97	FORM = 2 HO2 + CO	Photolysis	1.78E-5
98	FORM = CO + H2	Photolysis	2.38E-5
99	FORM + O = OH + HO2 + CO	k = 3.40E-11 exp(-1600/T)	1.58E-13
100	FORM + NO3 = HNO3 + HO2 + CO	k = 5.50E-16	5.50E-16
101	FORM + HO2 = HCO3	k = 9.70E-15 exp(625/T)	7.90E-14
102	HCO3 = FORM + HO2	k = 2.40E+12 exp(-7000/T)	1.51E+2
103	HCO3 + NO = FACD + NO2 + HO2	k = 5.60E-12	5.60E-12
104	HCO3 + HO2 = 0.5 MEPX + 0.5 FACD + 0.2 OH + 0.2 HO2	k = 5.60E-15 exp(2300/T)	1.26E-11
105	ALD2 + O = C2O3 + OH	k = 1.80E-11 exp(-1100/T)	4.49E-13
106	ALD2 + OH = C2O3	k = 4.70E-12 exp(345/T)	1.50E-11
107	ALD2 + NO3 = C2O3 + HNO3	k = 1.40E-12 exp(-1860/T)	2.73E-15
108	ALD2 = MEO2 + RO2 + CO + HO2	Photolysis	1.76E-6
109	ALDX + O = CXO3 + OH	k = 1.30E-11 exp(-870/T)	7.02E-13
110	ALDX + OH = CXO3	k = 4.90E-12 exp(405/T)	1.91E-11
111	ALDX + NO3 = CXO3 + HNO3	k = 6.30E-15	6.30E-15
112	ALDX = ALD2 + XO2H + RO2 + CO + HO2	Photolysis	6.96E-6
113	GLYD + OH = 0.2 GLY + 0.2 HO2 + 0.8 C2O3	k = 8.00E-12	8.00E-12

No.	Reactants and Products	Rate Constant Expression	k_{298}
114	GLYD = 0.74 FORM + 0.89 CO + 1.4 HO2 + 0.15 MEOH + 0.19 OH + 0.11 GLY + 0.11 XO2H + 0.11 RO2	Photolysis	1.56E-6
115	GLYD + NO3 = HNO3 + C2O3	k = 1.40E-12 exp(-1860/T)	2.73E-15
116	GLY + OH = 1.8 CO + 0.2 XO2 + 0.2 RO2 + HO2	k = 3.10E-12 exp(340/T)	9.70E-12
117	GLY = 2 HO2 + 2 CO	Photolysis	5.50E-5
118	GLY + NO3 = HNO3 + 1.5 CO + 0.5 XO2 + 0.5 RO2 + HO2	k = 1.40E-12 exp(-1860/T)	2.73E-15
119	MGLY = C2O3 + HO2 + CO	Photolysis	1.46E-4
120	MGLY + NO3 = HNO3 + C2O3 + XO2 + RO2	k = 1.40E-12 exp(-1860/T)	2.73E-15
121	MGLY + OH = C2O3 + CO	k = 1.90E-12 exp(575/T)	1.31E-11
122	H2 + OH = HO2	k = 7.70E-12 exp(-2100/T)	6.70E-15
123	CO + OH = HO2	k = k1 + k2 [M] k1 = 1.44E-13 k2 = 3.43E-33	2.28E-13
124	CH4 + OH = MEO2 + RO2	k = 1.85E-12 exp(-1690/T)	6.37E-15
125	ETHA + OH = 0.991 ALD2 + 0.991 XO2H + 0.009 XO2N + RO2	k = 6.90E-12 exp(-1000/T)	2.41E-13
126	MEOH + OH = FORM + HO2	k = 2.85E-12 exp(-345/T)	8.95E-13
127	ETOH + OH = 0.95 ALD2 + 0.9 HO2 + 0.1 XO2H + 0.1 RO2 + 0.078 FORM + 0.011 GLYD	k = 3.00E-12 exp(20/T)	3.21E-12
128	KET = 0.5 ALD2 + 0.5 C2O3 + 0.5 XO2H + 0.5 CXO3 + 0.5 MEO2 + RO2 - 2.5 PAR	Photolysis	2.27E-7
129	ACET = 0.38 CO + 1.38 MEO2 + 1.38 RO2 + 0.62 C2O3	Photolysis	2.08E-7
130	ACET + OH = FORM + C2O3 + XO2 + RO2	k = 1.41E-12 exp(-620.6/T)	1.76E-13
131	PRPA + OH = 0.71 ACET + 0.26 ALDX + 0.26 PAR + 0.97 XO2H + 0.03 XO2N + RO2	k = 7.60E-12 exp(-585/T)	1.07E-12
132	PAR + OH = 0.11 ALDX + 0.76 ROR + 0.13 XO2N + 0.11 XO2H + 0.76 XO2 + RO2 - 0.11 PAR	k = 8.10E-13	8.10E-13
133	ROR = 0.2 KET + 0.42 ACET + 0.74 ALD2 + 0.37 ALDX + 0.04 XO2N + 0.94 XO2H + 0.98 RO2 + 0.02 ROR - 2.7 PAR	k = 5.70E+12 exp(-5780/T)	2.15E+4
134	ROR + O2 = KET + HO2	k = 1.50E-14 exp(-200/T)	7.67E-15
135	ROR + NO2 = NTR1	k = 8.60E-12 exp(400/T)	3.29E-11
136	ETHY + OH = 0.7 GLY + 0.7 OH + 0.3 FACD + 0.3 CO + 0.3 HO2	Falloff: F=0.37; n=1.3 k(0) = 5.00E-30 (T/300)^-1.5 k(inf) = 1.00E-12	7.52E-13
137	ETH + O = FORM + HO2 + CO + 0.7 XO2H + 0.7 RO2 + 0.3 OH	k = 1.04E-11 exp(-792/T)	7.29E-13
138	ETH + OH = XO2H + RO2 + 1.56 FORM + 0.22 GLYD	Falloff: F=0.48; n=1.15 k(0) = 8.60E-29 (T/300)^-3.1 k(inf) = 9.00E-12 (T/300)^-0.85	7.84E-12
139	ETH + O3 = FORM + 0.51 CO + 0.16 HO2 + 0.16 OH + 0.37 FACD	k = 9.10E-15 exp(-2580/T)	1.58E-18
140	ETH + NO3 = 0.5 NO2 + 0.5 NTR1 + 0.5 XO2H + 0.5 XO2 + RO2 + 1.125 FORM	k = 3.30E-12 exp(-2880/T)	2.10E-16
141	OLE + O = 0.2 ALD2 + 0.3 ALDX + 0.1 HO2 + 0.2 XO2H + 0.2 CO + 0.2 FORM + 0.01 XO2N + 0.21 RO2 + 0.2 PAR + 0.1 OH	k = 1.00E-11 exp(-280/T)	3.91E-12

No.	Reactants and Products	Rate Constant Expression	k_{298}
142	OLE + OH = 0.781 FORM + 0.488 ALD2 + 0.488 ALDX + 0.976 XO2H + 0.195 XO2 + 0.024 XO2N + 1.195 RO2 - 0.73 PAR	Falloff: F=0.5; n=1.13 k(0) = 8.00E-27 (T/300)^-3.5 k(inf) = 3.00E-11 (T/300)^-1	2.86E-11
143	OLE + O3 = 0.295 ALD2 + 0.555 FORM + 0.27 ALDX + 0.15 XO2H + 0.15 RO2 + 0.334 OH + 0.08 HO2 + 0.378 CO + 0.075 GLY + 0.075 MGLY + 0.09 FACD + 0.13 AACD + 0.04 H2O2 - 0.79 PAR	k = 5.50E-15 exp(-1880/T)	1.00E-17
144	OLE + NO3 = 0.5 NO2 + 0.5 NTR1 + 0.48 XO2 + 0.48 XO2H + 0.04 XO2N + RO2 + 0.5 FORM + 0.25 ALD2 + 0.375 ALDX - 1 PAR	k = 4.60E-13 exp(-1155/T)	9.54E-15
145	IOLE + O = 1.24 ALD2 + 0.66 ALDX + 0.1 XO2H + 0.1 RO2 + 0.1 CO + 0.1 PAR	k = 2.30E-11	2.30E-11
146	IOLE + OH = 1.3 ALD2 + 0.7 ALDX + XO2H + RO2	k = 1.05E-11 exp(519/T)	5.99E-11
147	IOLE + O3 = 0.732 ALD2 + 0.442 ALDX + 0.128 FORM + 0.245 CO + 0.5 OH + 0.3 XO2H + 0.3 RO2 + 0.24 GLY + 0.06 MGLY + 0.29 PAR + 0.08 AACD + 0.08 H2O2	k = 4.70E-15 exp(-1013/T)	1.57E-16
148	IOLE + NO3 = 0.5 NO2 + 0.5 NTR1 + 0.48 XO2 + 0.48 XO2H + 0.04 XO2N + RO2 + 0.5 ALD2 + 0.625 ALDX + PAR	k = 3.70E-13	3.70E-13
149	ISOP + OH = ISO2 + RO2	k = 2.70E-11 exp(390/T)	9.99E-11
150	ISOP + O = 0.75 ISPD + 0.5 FORM + 0.25 XO2 + 0.25 RO2 + 0.25 HO2 + 0.25 CXO3 + 0.25 PAR	k = 3.00E-11	3.00E-11
151	ISO2 + NO = 0.1 INTR + 0.9 NO2 + 0.673 FORM + 0.9 ISPD + 0.818 HO2 + 0.082 XO2H + 0.082 RO2	k = 2.39E-12 exp(365/T)	8.13E-12
152	ISO2 + HO2 = 0.88 ISPX + 0.12 OH + 0.12 HO2 + 0.12 FORM + 0.12 ISPD	k = 7.43E-13 exp(700/T)	7.78E-12
153	ISO2 + C2O3 = 0.598 FORM + 1 ISPD + 0.728 HO2 + 0.072 XO2H + 0.8 MEO2 + 0.2 AACD + 0.872 RO2	k = k(ref) K k(ref) = k(58) K = 1.00E+0	1.30E-11
154	ISO2 + RO2 = 0.598 FORM + 1 ISPD + 0.728 HO2 + 0.072 XO2H + 0.072 RO2	k = k(ref) K k(ref) = k(70) K = 1.00E+0	3.48E-13
155	ISO2 = HO2 + HPLD	k = 3.30E+9 exp(-8300/T)	2.64E-3
156	ISOP + O3 = 0.6 FORM + 0.65 ISPD + 0.15 ALDX + 0.2 CXO3 + 0.35 PAR + 0.266 OH + 0.2 XO2 + 0.2 RO2 + 0.066 HO2 + 0.066 CO	k = 1.03E-14 exp(-1995/T)	1.27E-17
157	ISOP + NO3 = 0.35 NO2 + 0.65 NTR2 + 0.64 XO2H + 0.33 XO2 + 0.03 XO2N + RO2 + 0.35 FORM + 0.35 ISPD	k = 3.03E-12 exp(-448/T)	6.74E-13
158	ISPD + OH = 0.022 XO2N + 0.521 XO2 + 0.115 MGLY + 0.115 MEO2 + 0.269 GLYD + 0.269 C2O3 + 0.457 OPO3 + 0.117 PAR + 0.137 ACET + 0.137 CO + 0.137 HO2 + 0.658 RO2	k = 5.58E-12 exp(511/T)	3.10E-11
159	ISPD + O3 = 0.04 ALD2 + 0.231 FORM + 0.531 MGLY + 0.17 GLY + 0.17 ACET + 0.543 CO + 0.461 OH + 0.15 FACD + 0.398 HO2 + 0.143 C2O3	k = 3.88E-15 exp(-1770/T)	1.02E-17

No.	Reactants and Products	Rate Constant Expression	k_{298}
160	ISPD + NO3 = 0.717 HNO3 + 0.142 NTR2 + 0.142 NO2 + 0.142 XO2 + 0.142 XO2H + 0.113 GLYD + 0.113 MGLY + 0.717 PAR + 0.717 CXO3 + 0.284 RO2	k = 4.10E-12 exp(-1860/T)	7.98E-15
161	ISPD = 0.76 HO2 + 0.34 XO2H + 0.16 XO2 + 0.34 MEO2 + 0.208 C2O3 + 0.26 FORM + 0.24 OLE + 0.24 PAR + 0.17 ACET + 0.128 GLYD + 0.84 RO2	Photolysis	1.60E-5
162	ISPX + OH = 0.904 EPOX + 0.933 OH + 0.067 ISO2 + 0.067 RO2 + 0.029 IOLE + 0.029 ALDX	k = 2.23E-11 exp(372/T)	7.77E-11
163	HPLD = OH + ISPD	Photolysis	4.41E-4
164	HPLD + NO3 = HNO3 + ISPD	k = 6.00E-12 exp(-1860/T)	1.17E-14
165	EPOX + OH = EPX2 + RO2	k = 5.78E-11 exp(-400/T)	1.51E-11
166	EPX2 + HO2 = 0.275 GLYD + 0.275 GLY + 0.275 MGLY + 1.125 OH + 0.825 HO2 + 0.375 FORM + 0.074 FACD + 0.251 CO + 2.175 PAR	k = 7.43E-13 exp(700/T)	7.78E-12
167	EPX2 + NO = 0.275 GLYD + 0.275 GLY + 0.275 MGLY + 0.125 OH + 0.825 HO2 + 0.375 FORM + NO2 + 0.251 CO + 2.175 PAR	k = 2.39E-12 exp(365/T)	8.13E-12
168	EPX2 + C2O3 = 0.22 GLYD + 0.22 GLY + 0.22 MGLY + 0.1 OH + 0.66 HO2 + 0.3 FORM + 0.2 CO + 1.74 PAR + 0.8 MEO2 + 0.2 AACD + 0.8 RO2	k = k(ref) K k(ref) = k(58) K = 1.00E+0	1.30E-11
169	EPX2 + RO2 = 0.275 GLYD + 0.275 GLY + 0.275 MGLY + 0.125 OH + 0.825 HO2 + 0.375 FORM + 0.251 CO + 2.175 PAR + RO2	k = k(ref) K k(ref) = k(70) K = 1.00E+0	3.48E-13
170	INTR + OH = 0.63 XO2 + 0.37 XO2H + RO2 + 0.444 NO2 + 0.185 NO3 + 0.104 INTR + 0.592 FORM + 0.331 GLYD + 0.185 FACD + 2.7 PAR + 0.098 OLE + 0.078 ALDX + 0.266 NTR2	k = 3.10E-11	3.10E-11
171	TERP + O = 0.15 ALDX + 5.12 PAR	k = 3.60E-11	3.60E-11
172	TERP + OH = 0.75 XO2H + 0.5 XO2 + 0.25 XO2N + 1.5 RO2 + 0.28 FORM + 1.66 PAR + 0.47 ALDX	k = 1.50E-11 exp(449/T)	6.77E-11
173	TERP + O3 = 0.57 OH + 0.07 XO2H + 0.69 XO2 + 0.18 XO2N + 0.94 RO2 + 0.24 FORM + 0.001 CO + 7 PAR + 0.21 ALDX + 0.39 CXO3	k = 1.20E-15 exp(-821/T)	7.63E-17
174	TERP + NO3 = 0.47 NO2 + 0.28 XO2H + 0.75 XO2 + 0.25 XO2N + 1.28 RO2 + 0.47 ALDX + 0.53 NTR2	k = 3.70E-12 exp(175/T)	6.66E-12
175	BENZ + OH = 0.53 CRES + 0.352 BZO2 + 0.352 RO2 + 0.118 OPEN + 0.118 OH + 0.53 HO2	k = 2.30E-12 exp(-190/T)	1.22E-12
176	BZO2 + NO = 0.918 NO2 + 0.082 NTR2 + 0.918 GLY + 0.918 OPEN + 0.918 HO2	k = 2.70E-12 exp(360/T)	9.04E-12
177	BZO2 + C2O3 = GLY + OPEN + HO2 + MEO2 + RO2	k = k(ref) K k(ref) = k(58) K = 1.00E+0	1.30E-11
178	BZO2 + HO2 =	k = 1.90E-13 exp(1300/T)	1.49E-11
179	BZO2 + RO2 = GLY + OPEN + HO2 + RO2	k = k(ref) K k(ref) = k(70) K = 1.00E+0	3.48E-13
180	TOL + OH = 0.18 CRES + 0.65 TO2 + 0.72 RO2 + 0.1 OPEN + 0.1 OH + 0.07 XO2H + 0.18 HO2	k = 1.80E-12 exp(340/T)	5.63E-12

No.	Reactants and Products	Rate Constant Expression	k_{298}
181	TO2 + NO = 0.86 NO2 + 0.14 NTR2 + 0.417 GLY + 0.443 MGLY + 0.66 OPEN + 0.2 XOPN + 0.86 HO2	k = 2.70E-12 exp(360/T)	9.04E-12
182	TO2 + C2O3 = 0.48 GLY + 0.52 MGLY + 0.77 OPEN + 0.23 XOPN + HO2 + MEO2 + RO2	k = k(ref) K k(ref) = k(58) K = 1.00E+0	1.30E-11
183	TO2 + HO2 =	k = 1.90E-13 exp(1300/T)	1.49E-11
184	TO2 + RO2 = 0.48 GLY + 0.52 MGLY + 0.77 OPEN + 0.23 XOPN + HO2 + RO2	k = k(ref) K k(ref) = k(70) K = 1.00E+0	3.48E-13
185	XYL + OH = 0.155 CRES + 0.544 XLO2 + 0.602 RO2 + 0.244 XOPN + 0.244 OH + 0.058 XO2H + 0.155 HO2	k = 1.85E-11	1.85E-11
186	XLO2 + NO = 0.86 NO2 + 0.14 NTR2 + 0.221 GLY + 0.675 MGLY + 0.3 OPEN + 0.56 XOPN + 0.86 HO2	k = 2.70E-12 exp(360/T)	9.04E-12
187	XLO2 + HO2 =	k = 1.90E-13 exp(1300/T)	1.49E-11
188	XLO2 + C2O3 = 0.26 GLY + 0.77 MGLY + 0.35 OPEN + 0.65 XOPN + HO2 + MEO2 + RO2	k = k(ref) K k(ref) = k(58) K = 1.00E+0	1.30E-11
189	XLO2 + RO2 = 0.26 GLY + 0.77 MGLY + 0.35 OPEN + 0.65 XOPN + HO2 + RO2	k = k(ref) K k(ref) = k(70) K = 1.00E+0	3.48E-13
190	CRES + OH = 0.025 GLY + 0.025 OPEN + HO2 + 0.2 CRO + 0.732 CAT1 + 0.02 XO2N + 0.02 RO2	k = 1.70E-12 exp(950/T)	4.12E-11
191	CRES + NO3 = 0.3 CRO + HNO3 + 0.48 XO2 + 0.12 XO2H + 0.24 GLY + 0.24 MGLY + 0.48 OPO3 + 0.1 XO2N + 0.7 RO2	k = 1.40E-11	1.40E-11
192	CRO + NO2 = CRON	k = 2.10E-12	2.10E-12
193	CRO + HO2 = CRES	k = 5.50E-12	5.50E-12
194	CRON + OH = NTR2 + 0.5 CRO	k = 1.53E-12	1.53E-12
195	CRON + NO3 = NTR2 + 0.5 CRO + HNO3	k = 3.80E-12	3.80E-12
196	CRON = HONO + HO2 + FORM + OPEN	Photolysis	9.45E-5
197	XOPN = 0.4 GLY + XO2H + 0.7 HO2 + 0.7 CO + 0.3 C2O3	Photolysis	5.04E-4
198	XOPN + OH = MGLY + 0.4 GLY + 2 XO2H + 2 RO2	k = 9.00E-11	9.00E-11
199	XOPN + O3 = 1.2 MGLY + 0.5 OH + 0.6 C2O3 + 0.1 ALD2 + 0.5 CO + 0.3 XO2H + 0.3 RO2	k = 1.08E-16 exp(-500/T)	2.02E-17
200	XOPN + NO3 = 0.5 NO2 + 0.5 NTR2 + 0.45 XO2H + 0.45 XO2 + 0.1 XO2N + RO2 + 0.25 OPEN + 0.25 MGLY	k = 3.00E-12	3.00E-12
201	OPEN = OPO3 + HO2 + CO	Photolysis	5.04E-4
202	OPEN + OH = 0.6 OPO3 + 0.4 XO2H + 0.4 RO2 + 0.4 GLY	k = 4.40E-11	4.40E-11
203	OPEN + O3 = 1.4 GLY + 0.24 MGLY + 0.5 OH + 0.12 C2O3 + 0.08 FORM + 0.02 ALD2 + 1.98 CO + 0.56 HO2	k = 5.40E-17 exp(-500/T)	1.01E-17
204	OPEN + NO3 = OPO3 + HNO3	k = 3.80E-12	3.80E-12
205	CAT1 + OH = 0.14 FORM + 0.2 HO2 + 0.5 CRO	k = 5.00E-11	5.00E-11
206	CAT1 + NO3 = CRO + HNO3	k = 1.70E-10	1.70E-10
207	OPO3 + NO = NO2 + 0.5 GLY + 0.5 CO + 0.8 HO2 + 0.2 CXO3	k = 1.00E-11	1.00E-11

No.	Reactants and Products	Rate Constant Expression	k_{298}
208	OPO3 + NO2 = OPAN	k = k(ref) K k(ref) = k(54) K = 1.00E+0	9.40E-12
209	OPAN = OPO3 + NO2	k = k(ref) K k(ref) = k(55) K = 1.00E+0	2.98E-4
210	OPO3 + HO2 = 0.41 PACD + 0.15 AACD + 0.15 O3 + 0.44 ALDX + 0.44 XO2H + 0.44 RO2 + 0.44 OH	k = k(ref) K k(ref) = k(57) K = 1.00E+0	1.39E-11
211	OPO3 + C2O3 = MEO2 + XO2 + ALDX + 2 RO2	k = k(ref) K k(ref) = k(59) K = 1.00E+0	1.55E-11
212	OPO3 + RO2 = 0.8 XO2H + 0.8 ALDX + 1.8 RO2 + 0.2 AACD	k = k(ref) K k(ref) = k(58) K = 1.00E+0	1.30E-11
213	OPAN + OH = 0.5 NO2 + 0.5 GLY + CO + 0.5 NTR2	k = 3.60E-11	3.60E-11
214	PANX + OH = ALD2 + NO2	k = 3.00E-12	3.00E-12
215	NTR2 = HNO3	k = 2.30E-5	2.30E-5
216	ECH4 + OH = MEO2 + RO2	k = 1.85E-12 exp(-1690/T)	6.37E-15

Notes:

k_{298} is the rate constant at 298 K and 1 atmosphere using units molecules cm^{-3} and s^{-1}

For photolysis reactions k_{298} shows the photolysis rate at a solar zenith angle of 60° and height of 600 m agl

Rate constant expressions are explained in the CAMx User's Guide

Table 2-2. Chemical species included in CB6r2.

Species	Description
BZO2	Peroxy radical from OH addition to benzene
C2O3	Acetylperoxy radical
CRO	Alkoxy radical from cresol
CXO3	C3 and higher acylperoxy radicals
ECH4	Emitted methane (over and above the background CH4)
EPX2	Peroxy radical from EPOX reaction with OH
HCO3	Adduct from HO2 plus formaldehyde
HO2	Hydroperoxy radical
ISO2	Peroxy radical from OH addition to isoprene
MEO2	Methylperoxy radical
NO3	Nitrate radical
O	Oxygen atom in the O3(P) electronic state
O1D	Oxygen atom in the O1(D) electronic state
OH	Hydroxyl radical
OPO3	Peroxyacyl radical from OPEN
RO2	Operator to approximate total peroxy radical concentration
ROR	Secondary alkoxy radical
TO2	Peroxy radical from OH addition to TOL
XLO2	Peroxy radical from OH addition to XYL
XO2	NO to NO2 conversion from alkylperoxy (RO2) radical
XO2H	NO to NO2 conversion (XO2) accompanied by HO2 production
XO2N	NO to organic nitrate conversion from alkylperoxy (RO2) radical
AACD	Acetic acid
ACET	Acetone
ALD2	Acetaldehyde
ALDX	Propionaldehyde and higher aldehydes
BENZ	Benzene
CAT1	Methyl-catechols
CO	Carbon monoxide
CRES	Cresols
CRON	Nitro-cresols
EPOX	Epoxide formed from ISPX reaction with OH
ETH	Ethene
ETHA	Ethane
ETHY	Ethyne
ETOH	Ethanol
FACD	Formic acid
FORM	Formaldehyde
GLY	Glyoxal
GLYD	Glycolaldehyde
H2O2	Hydrogen peroxide
HNO3	Nitric acid
HONO	Nitrous acid
HPLD	hydroperoxyaldehyde
INTR	Organic nitrates from ISO2 reaction with NO
IOLE	Internal olefin carbon bond (R-C=C-R)
ISOP	Isoprene
ISPD	Isoprene product (lumped methacrolein, methyl vinyl ketone, etc.)

Species	Description
ISPX	Hydroperoxides from ISO2 reaction with HO2
KET	Ketone carbon bond (C=O)
MEOH	Methanol
MEPX	Methylhydroperoxide
MGLY	Methylglyoxal
N2O5	Dinitrogen pentoxide
NO	Nitric oxide
NO2	Nitrogen dioxide
NTR1	Simple organic nitrates
NTR2	Multi-functional organic nitrates
O3	Ozone
OLE	Terminal olefin carbon bond (R-C=C)
OPAN	Peroxyacyl nitrate (PAN compound) from OPO3
OPEN	Aromatic ring opening product (unsaturated dicarbonyl)
PACD	Peroxyacetic and higher peroxycarboxylic acids
PAN	Peroxyacetyl Nitrate
PANX	C3 and higher peroxyacyl nitrate
PAR	Paraffin carbon bond (C-C)
PNA	Peroxynitric acid
PRPA	Propane
ROOH	Higher organic peroxide
SO2	Sulfur dioxide
SULF	Sulfuric acid (gaseous)
TERP	Monoterpenes
TOL	Toluene and other monoalkyl aromatics
XOPN	Aromatic ring opening product (unsaturated dicarbonyl)
XYL	Xylene and other polyalkyl aromatics
CH4	Methane background (set within CAMx to 1.75 ppm)
H2	Hydrogen (set within CAMx to 0.6 ppm)
M	Third body gas (set within CAMx based on atmospheric density)
O2	Oxygen (set within CAMx to 0.2 M)
H2O	Water vapor (set within CAMx based on humidity)

2.2 Halogen Chemistry

2.2.1 Chlorine Mechanism

The chlorine (Cl) reaction mechanism is based on Koo et al. (2012) with the following updates:

- Reaction rate constants updated to IUPAC (2014a and b) as necessary
- Species names changed to be consistent with the Br and I mechanisms as necessary
- Cl-atoms with organic compounds are limited to alkanes and isoprene
- Added ClO radical reactions with BrO and IO
- Added $ClNO_3$ hydrolysis to HOCl on aerosols
- Cl-atom reactions with organic compounds limited to alkanes and isoprene

- Added Cl-atom production from photolysis of certain chloromethanes (CH_2BrCl, $CHBr_2Cl$, $CHBrCl_2$) included

Reactions of Cl-atoms with organic compounds are limited to alkanes and isoprene. Alkanes can dominate Cl-atom removal by anthropogenic organic compounds because Cl-atoms react rapidly with light alkanes (1.4×10^{-10} cm^{-3} $molecule^{-1}$ s^{-1} for propane and 1.6×10^{-11} cm^{-3} $molecule^{-1}$ s^{-1} for ethane) and light alkanes are ubiquitous and abundant because they have large emissions and react slowly with OH radical (1×10^{-12} cm^{-3} $molecule^{-1}$ s^{-1} for propane and 2.5×10^{-13} cm^{-3} $molecule^{-1}$ s^{-1} for ethane). The reaction of Cl-atoms with isoprene is included to account for the influence of biogenic emissions on Cl-atom removal.

Cl-atom production from the photolysis of chloromethanes is included only for those halomethanes that are included as sources of Br (i.e., CH_2BrCl, $CHBr_2Cl$, $CHBrCl_2$) from seawater. Degradation of anthropogenic chlorocarbons (e.g., HCFCs) is not included in the mechanism but could be added to study the influence on regional ozone.

The relationships between species in the chlorine mechanism are diagramed in Figure 2-1 and the mechanism is listed in Section 2.2.4.

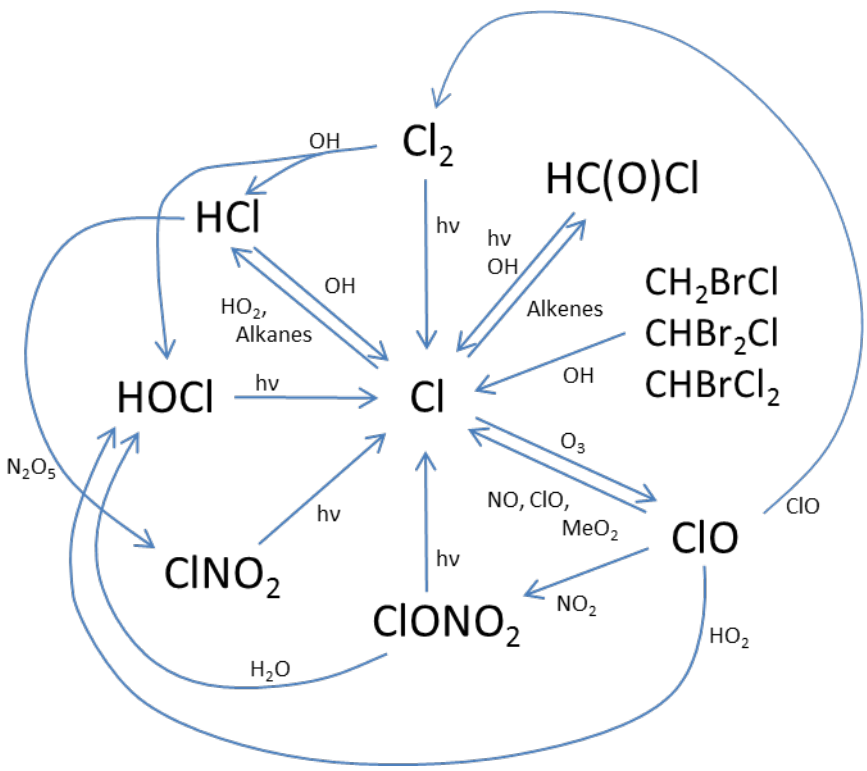

Figure 2-1. Relationships between chemical species in the Cl mechanism.

The dominant source of atmospheric Cl influencing Texas is expected to be sea salt emissions from the Gulf of Mexico. Hydrochloric acid (HCl) is displaced into the gas phase when sea salt aerosols are acidified by nitric and sulfuric acids. The HCl formed from sea salt can react with dinitrogen pentoxide (N_2O_5) on aerosol surfaces to produce nitryl chloride ($ClNO_2$) which photolyzes to produces Cl-atoms. If aerosols are modeled explicitly in CAMx then HCl production from sea salt and subsequent formation of $ClNO_2$ are explicitly modeled by the CAMx aerosol module (Koo et al., 2012.) For cases where aerosol chemistry is not modeled, the Cl mechanism includes two pseudo gas-phase reactions:

SSCl + HNO3 --> HCL + SSN3

HCL + N2O5 --> CLN2 + HNO3

The Cl-content of sea salt aerosol is represented by the pseudo gas-phase species SSCL which reacts with nitric acid (HNO_3) to form HCl and a pseudo gas-phase species for sodium nitrate (SSN3). The reaction of HCl with N_2O_5 is represented as a gas gas-phase reaction. Representative rate constants are used for both of these pseudo gas-phase reactions. Hydrolysis of $ClNO_3$ is included as pseudo gas-phase reaction with a rate constant comparable to hydrolysis of N_2O_5.

Atmospheric reactions of Cl-atoms can produce or destroy tropospheric O_3. When Cl-atoms react with VOCs such as alkanes and isoprene they can initiate O_3 formation by reactions similar to those initiated by OH. Cl-atoms can destroy O_3through series of chemical reactions such as the ClO + HO_2 cycle shown below.

	ClO + HO_2 cycle	*ClO + ClO cycle*	*$ClNO_3$ + H_2O cycle*
	$Cl + O_3 \rightarrow ClO + O_2$	$(Cl + O_3 \rightarrow ClO + O_2) \times 2$	$Cl + O_3 \rightarrow ClO + O_2$
	$ClO + HO_2 \rightarrow HOCl + O_2$	$ClO + ClO \rightarrow Cl_2 + O_2$	$ClO + NO_2 \rightarrow ClNO_3$
	$HOCl + h\nu \rightarrow Cl + OH$	$Cl_2 \rightarrow 2\ Cl$	$ClNO_3 + H_2O$ −aer $\rightarrow HOCl + HNO_3$
			$HOCl + h\nu \rightarrow Cl + OH$
Net:	$O_3 + HO_2 \rightarrow OH + 2\ O_2$	$2\ O_3 \rightarrow 3\ O_2$	$O_3 + NO_2 + H_2O \rightarrow O_2 + HNO_3 + OH$

The net effect of each set of reactions is O_3 conversion to O_2 along with other changes. These sets of reactions are referred to as catalytic cycles because the Cl-atom is regenerated in the reactions and therefore one Cl-atom can potentially destroy many O_3 molecules. Cl-atoms and chlorine monoxide (ClO) are rapidly interconverted by these reactions such that is useful to consider them collectively (Cl + ClO) as reactive Cl. Catalytic destruction of O_3 by Cl is interrupted when reactive Cl is converted to a reservoir species such as HCl, HOCl, $ClNO_2$, $ClNO_3$ or HC(O)Cl (Figure 2-1). However, Cl can be returned from each of these reservoir species back to reactive Cl. Therefore, catalytic destruction of O_3 by Cl is terminated only when deposition removes reservoir species, e.g., by dry or wet deposition of HCl.

2.2.2 Bromine Mechanism

A literature survey identified several chemical mechanisms that have been used to model the influence of bromine (Br) chemistry on atmospheric oxidants:

Vogt et al. (1999) implemented Br, Cl and I chemistry in a box model to study halogen chemistry in the marine boundary layer.

Yang et al. (2005) implemented bromine chemistry in a global modelto study the effect of Br from bromocarbon degradation and from sea-salt aerosols on ozone and oxidants.

Whitten and Yarwood (2008) studied regional ozone formation and destruction from the potential use of n-propyl bromide (C_3H_7Br) as an industrial solvent by adding Br chemistry to the CB4 chemical mechanism.

Smoydzin and von Glasow (2009) modeled the influence of Br chemistry on ozone near the Dead Sea.

Ordóñez et al. (2012) studied the influence of very short lived bromine and iodine compounds on global oxidants and implemented a chemical mechanism for bromine and iodine.

Parrella et al. (2012) implemented bromine chemistry in the GEOS-Chem global model and found improved simulations of global ozone and mercury.

The Br reaction mechanism is similar to the mechanisms of Yang et al. (2005), Smoydzin and von Glasow (2009) and Parrella et al. (2012) and is more compact than the mechanisms of Vogt et al. (1999), Whitten and Yarwood (2008) and Ordóñez et al. (2012). Reaction rate constants for the Br mechanism are from IUPAC (2014a and b) and species names were chosen to be consistent with the Cl and I mechanisms. Reactions of BrO with ClO and IO are included to interconnect the mechanisms for different halogens. Hydrolysis of $BrNO_3$ is included as pseudo gas-phase reaction with a rate constant comparable to hydrolysis of N_2O_5. The relationships between species in the Br mechanism are diagramed in Figure 2-2 and the mechanism is listed in Section 2.2.4.

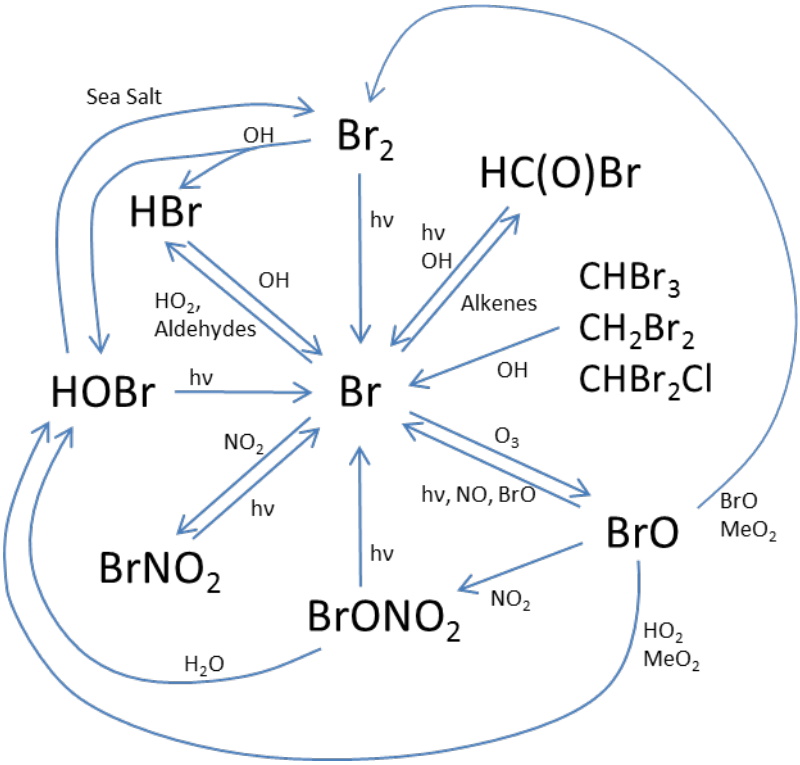

Figure 2-2. Relationships between chemical species in the Br mechanism.

The largest source of atmospheric Br is sea salt aerosol (Yang et al., 2005) although the mechanism by which sea salt Br enters the gas-phase (Br depletion of sea salt aerosol) differs from that for Cl depletion of sea salt under acid conditions (discussed above). Br depletion of sea salt aerosol occurs when HOBr interacts with sea salt to form Br_2 and this mechanism can occur at neutral as well as acid pH. This mechanism is implemented as a pseudo gas-phase reaction:

SSBR + HOBr --> Br2

Other sources of atmospheric Br included in the mechanism are decomposition of the halomethanes $CHBr_3$, CH_2Br_2, CH_2BrCl, $CHBr_2Cl$ and $CHBrCl_2$.

Atmospheric reactions of Br-atoms can destroy tropospheric O_3 through series of chemical reactions such as the BrO + HO2 cycle shown below.

	BrO + HO_2 cycle	*$BrNO_3$ + H_2O cycle*	*HOBr + HBr cycle*
	$Br + O_3 \rightarrow BrO + O_2$	$Br + O_3 \rightarrow BrO + O_2$	$Br + O_3 \rightarrow BrO + O_2$
	$BrO + HO_2 \rightarrow HOBr + O_2$	$BrO + NO_2 \rightarrow BrNO_3$	$BrO + HO_2 \rightarrow HOBr + O_2$
	$\underline{HOBr + hv \rightarrow Br + OH}$	$BrNO_3 + H_2O$ –aer $\rightarrow HOBr + HNO_3$	$Br + R\text{-}H \rightarrow HBr + R$
		$\underline{HOBr + hv \rightarrow Br + OH}$	$HOBr + HBr$ –aer$\rightarrow Br_2 + H_2O$
			$\underline{Br_2 \rightarrow 2\ Br}$
Net	$O_3 + HO_2 \rightarrow OH + 2\ O_2$	$O_3 + NO_2 + H_2O \rightarrow O_2 + HNO_3 + OH$	$O_3 + HO_2 + R\text{-}H \rightarrow 2\ O_2 + H_2O + R$

These sets of reactions are referred to as catalytic cycles because the Br-atom is regenerated in the reactions and therefore one Br-atom can potentially destroy many O_3 molecules. Br-atoms and bromine monoxide (BrO) are rapidly interconverted by these reactions such that is useful to consider them collectively (Br + BrO) as reactive Br. Catalytic destruction of O_3 by Br is interrupted when reactive Br is converted to a reservoir species such as HBr, HOBr, $BrNO_2$ or $BrNO_3$ (Figure 2-2). However, Br can be returned from each of these reservoir species to back to reactive Br. Therefore, catalytic destruction of O_3 by Br is terminated only when deposition removes reservoir species, e.g., by dry or wet deposition of HBr.

2.2.3 Iodine

The iodine (I) reaction mechanism is based on Yarwood et al. (2012) with the following updates:

- Reaction rate constants updated to IUPAC (2014a and b) as necessary
- Species names changed to be consistent with the Cl and Br mechanisms as necessary
- Added IO radical reactions with ClO and BrO
- Added INO_3 hydrolysis to HOI on aerosols
- Removed INO and related reactions

Reactions of IO with ClO and BrO are included to interconnect the mechanisms for different halogens. Reactions of INO were removed because INO concentrations were found to be small (Yarwood et al., 2012.) Hydrolysis of INO_3 is included as pseudo gas-phase reaction with a rate constant comparable to hydrolysis of N_2O_5. The relationships between species in the I mechanism are diagramed in Figure 2-3 and the mechanism is listed in Section 2.2.4.

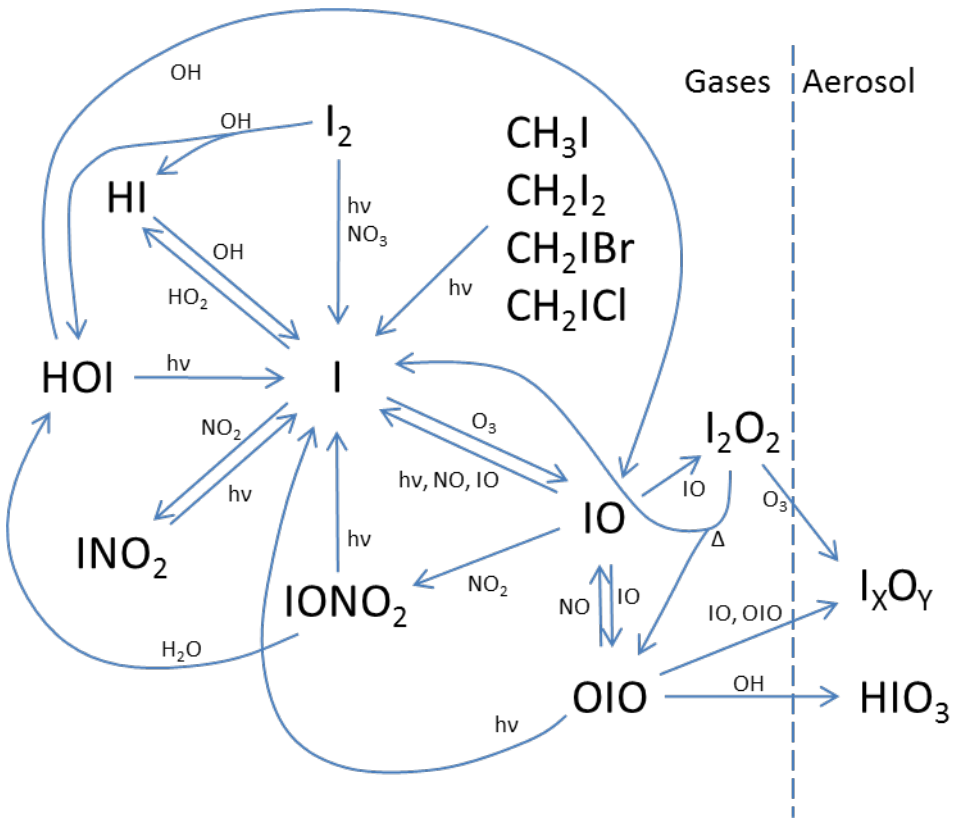

Figure 2-3. Relationships between chemical species in the I mechanism.

Atmospheric reactions of iodine atoms (I-atoms) can destroy tropospheric ozone through series of chemical reactions such as the IO + HO2 cycle (Chameides and Davis, 1980) shown below.

	IO + HO_2 cycle	*IO + IO cycle*	*IO + NO_2 cycle*
	$I + O_3 \rightarrow IO + O_2$	$(I + O_3 \rightarrow IO + O_2) \times 2$	$I + O_3 \rightarrow IO + O_2$
	$IO + HO_2 \rightarrow HOI + O_2$	$IO + IO \rightarrow I + OIO$	$IO + NO_2 \rightarrow IONO_2$
	$HOI + hv \rightarrow I + OH$	$OIO + hv \rightarrow I + O_2$	$IONO_2 + hv \rightarrow I + NO_3$
			$NO_3 + hv \rightarrow NO + O_2$
			$NO + O_3 \rightarrow NO_2 + O_2$
Net:	$O_3 + HO_2 \rightarrow OH + 2\ O_2$	$2\ O_3 \rightarrow 3\ O_2$	$2\ O_3 \rightarrow 3\ O_2$

These reactions are referred to as catalytic cycles because the I-atom is regenerated in the reactions and therefore one I-atom can potentially destroy many O_3 molecules. I-atoms and iodine monoxide (IO) are rapidly interconverted by these reactions such that is useful to consider them collectively (I + IO) as reactive iodine.

These sets of reactions are referred to as catalytic cycles because the I-atom is regenerated in the reactions and therefore one I-atom can potentially destroy many O_3 molecules. I-atoms and iodine monoxide (IO) are rapidly interconverted by these reactions such that is useful to

consider them collectively (I + IO) as reactive I. Catalytic destruction of O_3 by I is interrupted when reactive Br is converted to a reservoir species such as HI, HOI, INO_2 or INO_3 (Figure 2-3). However, I can be returned from each of these reservoir species to back to reactive I.

The atmospheric reactions of I differ from Br and Cl in several ways:

- I-atoms do not abstract H from organic compounds in contrast to Br and Cl-atoms
- Formation of oxides is more extensive for I (IO, OIO, I_2O_2, IxOy) than for Br (BrO) or Cl (ClO)
- Larger iodine oxides (IxOy) form aerosols whereas Cl and Br oxides remain in the gas phase.

Aerosol formation by larger iodine oxides is a sink for reactive I that can terminate O_3 destruction by reactive I.

2.2.4 Integrated Halogen Mechanism

The chemical reactions in the halogen mechanism are listed in Table 2-3 and the chemical species names are defined in Table 2-4. The halogen mechanism has 88 reactions and 41 species. When these halogen reactions are combined with CB6r2 the mechanism may be referred to as CB6r2h. CAMx simulations times with CB6r2h are about double those for CB6r2 when aerosols are not modeled explicitly.

Table 2-3. Reaction listing for the halogen mechanism.

No.	Reactants and Products	Rate Constant Expression	k_{298}
1	CL2 = 2 CL	Photolysis	1.56E-3
2	HOCL = CL + OH	Photolysis	1.34E-4
3	CL + O3 = CLO	k = 2.30E-11 exp(-200/T)	1.18E-11
4	CLO + CLO = 0.3 CL2 + 1.4 CL	k = 1.63E-14	1.63E-14
5	CLO + NO = CL + NO2	k = 6.40E-12 exp(290/T)	1.69E-11
6	CLO + HO2 = HOCL	k = 2.70E-12 exp(220/T)	5.65E-12
7	CLO + NO2 = CLN3	Falloff: F=0.6; n=1 k(0) = 1.80E-31 (T/300)^-3.4 k(inf) = 1.50E-11 (T/300)^-1.9	2.34E-12
8	CLN3 = CLO + NO2	Falloff: F=0.6; n=1 k(0) = 4.48E-5 (T/300)^-1 exp(-12530/T) k(inf) = 3.71E+15 (T/300)^3.5 exp(-12530/T)	3.11E-4
9	CLN3 = CLO + NO2	Photolysis	4.97E-6
10	CLN3 = CL + NO3	Photolysis	4.67E-4
11	CLN3 + H2O = HOCL + HNO3	k = 2.50E-22	2.50E-22
12	OH + HCL = CL	k = 6.58E-13 (T/300)^1.2 exp(58/T)	7.93E-13
13	OH + FMCL = CL + CO	k = 3.67E-11 exp(-1419/T)	3.14E-13
14	FMCL = CL + CO + HO2	Photolysis	6.10E-8
15	CLO + MEO2 = CL + FORM + HO2	k = 4.10E-13 exp(-800/T)	2.80E-14
16	CL + CH4 = HCL + MEO2	k = 6.60E-12 exp(-1240/T)	1.03E-13
17	CL + PAR = HCL	k = 5.00E-11	5.00E-11
18	CL + ETHA = HCL + 0.991 ALD2 + 0.991 XO2H + 0.009 XO2N + RO2	k = 8.30E-11 exp(-100/T)	5.93E-11
19	CL + PRPA = HCL + ACET + 0.97 XO2H + 0.03 XO2N + RO2	k = 1.40E-10	1.40E-10

No.	Reactants and Products	Rate Constant Expression	k_{298}
20	CL + ISOP = FMCL + ISPD + 0.96 XO2H + 0.04 XO2N + RO2	k = 4.30E-10	4.30E-10
21	HCL + N2O5 = CLN2 + HNO3	k = 6.00E-13	6.00E-13
22	CLN2 = CL + NO2	Photolysis	2.86E-4
23	BR2 = 2 BR	Photolysis	2.79E-2
24	HOBR = BR + OH	Photolysis	1.51E-3
25	BR2 + OH = HOBR + BR	k = 5.40E-11 exp(180/T)	9.88E-11
26	HBR + OH = BR	k = 5.50E-12 exp(-200/T)	2.81E-12
27	BR + O3 = BRO	k = 1.60E-11 exp(780/T)	2.19E-10
28	BR + HO2 = HBR	k = 4.80E-12 exp(310/T)	1.36E-11
29	BR + NO2 = BRN2	Falloff: F=0.6; n=1 k(0) = 4.20E-31 (T/300)^-2.4 k(inf) = 2.70E-11	4.89E-12
30	BR + NO3 = BRO + NO2	k = 1.60E-11	1.60E-11
31	BRO = BR + O	Photolysis	2.05E-2
32	BRO + HO2 = HOBR	k = 4.50E-12 exp(460/T)	2.11E-11
33	BRO + OH = BR + HO2	k = 1.70E-11 exp(250/T)	3.93E-11
34	BRO + BRO = 2 BR	k = 2.40E-12 exp(40/T)	2.74E-12
35	BRO + BRO = BR2	k = 2.80E-14 exp(860/T)	5.02E-13
36	BRO + NO = BR + NO2	k = 8.80E-12 exp(260/T)	2.11E-11
37	BRO + NO2 = BRN3	Falloff: F=0.6; n=1 k(0) = 5.20E-31 (T/300)^-3.2 k(inf) = 6.90E-12	2.81E-12
38	BRN2 = BR + NO2	Photolysis	3.21E-3
39	BRN3 = BR + NO3	Photolysis	9.76E-4
40	BRN3 + H2O = HOBR + HNO3	k = 2.50E-22	2.50E-22
41	FMBR + OH = BR + CO	k = 5.00E-12	5.00E-12
42	FMBR = BR + CO + HO2	Photolysis	4.15E-6
43	BRO + MEO2 = 0.75 HOBR + 0.25 BR + FORM	k = 4.10E-13 exp(-800/T)	2.80E-14
44	BR + FORM = HBR + CO + HO2	k = 7.70E-11 exp(-580/T)	1.10E-11
45	BR + ALD2 = HBR + C2O3	k = 1.80E-11 exp(-460/T)	3.84E-12
46	BR + OLE = FMBR + ALD2 + XO2H - 1 PAR + RO2	k = 3.60E-12	3.60E-12
47	BR + ISOP = FMBR + ISPD + 0.96 XO2H + 0.04 XO2N + RO2	k = 5.00E-12	5.00E-12
48	I2 = 2 I	Photolysis	1.30E-1
49	HOI = I + OH	Photolysis	6.36E-2
50	I2 + OH = I + HOI	k = 2.10E-10	2.10E-10
51	I2 + NO3 = I + INO3	k = 1.50E-12	1.50E-12
52	HI + OH = I	k = 1.60E-11 exp(440/T)	7.00E-11
53	I + O3 = IO	k = 2.10E-11 exp(-830/T)	1.30E-12
54	I + HO2 = HI	k = 1.50E-11 exp(-1090/T)	3.87E-13
55	I + NO2 = INO2	Falloff: F=0.63; n=1 k(0) = 3.00E-31 (T/300)^-1 k(inf) = 6.60E-11	5.24E-12
56	IO = I + O	Photolysis	1.18E-1
57	IO + IO = 0.4 I + 0.4 OIO + 0.6 I2O2	k = 5.40E-11 exp(180/T)	9.88E-11
58	IO + HO2 = HOI	k = 1.40E-11 exp(540/T)	8.57E-11
59	IO + NO = I + NO2	k = 7.15E-12 exp(300/T)	1.96E-11

No.	Reactants and Products	Rate Constant Expression	k_{298}
60	IO + NO2 = INO3	Falloff: F=0.4; n=1 k(0) = 7.70E-31 (T/300)^-5 k(inf) = 1.60E-11	3.55E-12
61	HOI + OH = IO	k = 5.00E-12	5.00E-12
62	OIO = I	Photolysis	1.28E-1
63	OIO + OH = HIO3	Falloff: F=0.3; n=1 k(0) = 1.50E-27 (T/300)^-3.93 k(inf) = 5.50E-10 exp(46/T)	4.72E-10
64	OIO + IO = IXOY	k = 1.00E-10	1.00E-10
65	OIO + OIO = IXOY	k = 1.50E-10	1.50E-10
66	OIO + NO = IO + NO2	k = 1.10E-12 exp(542/T)	6.78E-12
67	I2O2 = I + OIO	k = 1.00E+1	1.00E+1
68	I2O2 + O3 = IXOY	k = 1.00E-12	1.00E-12
69	INO2 = I + NO2	Photolysis	3.21E-3
70	INO2 + INO2 = I2 + 2 NO2	k = 4.70E-13 exp(-1670/T)	1.73E-15
71	INO3 = I + NO3	Photolysis	1.25E-2
72	INO3 + H2O = HOI + HNO3	k = 2.50E-22	2.50E-22
73	CLO + BRO = CL + BR	k = 4.70E-12 exp(320/T)	1.38E-11
74	CLO + IO = CL + I	k = 4.70E-12 exp(280/T)	1.20E-11
75	BRO + IO = BR + I	k = 1.50E-11 exp(510/T)	8.31E-11
76	CH3I = I + MEO2	Photolysis	3.19E-6
77	MI2 = 2 I + FORM	Photolysis	4.69E-3
78	MIB = I + BR + FORM	Photolysis	2.53E-4
79	MIC = I + CL + FORM	Photolysis	7.48E-5
80	MB3 = 3 BR + HO2 + CO	Photolysis	4.64E-7
81	MB3 + OH = 3 BR + CO	k = 1.35E-12 exp(-600/T)	1.80E-13
82	MB2 + OH = 2 BR + HO2 + CO	k = 2.00E-12 exp(-840/T)	1.19E-13
83	MBC + OH = BR + MEO2	k = 2.35E-12 exp(-1300/T)	3.00E-14
84	MBC2 + OH = BR + MEO2	k = 9.00E-13 exp(-600/T)	1.20E-13
85	MB2C + OH = BR + MEO2	k = 9.00E-13 exp(-600/T)	1.20E-13
86	IALK = I + ALDX + XO2H + RO2	Photolysis	5.88E-7
87	SSCL + HNO3 = HCL + SSN3	k = 1.00E-12	1.00E-12
88	SSBR + HOBR = BR2	k = 1.00E-12	1.00E-12

Notes:

k_{298} is the rate constant at 298 K and 1 atmosphere using units molecules cm^{-3} and s^{-1}

For photolysis reactions k_{298} shows the photolysis rate at a solar zenith angle of 60° and height of 600 m agl

Rate constant expressions are explained in the CAMx User's Guide

Table 2-4. Chemical species included in CB6r2.

Species	Description	Formula							Mol. Wt.
		C	H	O	N	Cl	Br	I	
CL2	Molecular chlorine					2			70.9
CL	Chlorine atom					1			35.5
CLO	Chlorine monoxide			1		1			51.4
HCL	Hydrogen chloride		1			1			36.5
HOCL	Hypochlorous acid		1	1		1			52.4
CLN2	Nitryl chloride: $ClNO_2$			2		1			81.4
CLN3	Chlorine nitrate: $ClONO_2$			3		1			97.4
FMCL	Formyl chloride: HC(O)Cl	1	1	1		1			64.5
BR2	Molecular bromine						2		159.8
BR	Bromine atom						1		79.9
BRO	Bromine monoxide			1			1		95.9
HBR	Hydrogen bromide		1				1		80.9
HOBR	Hypobromous acid		1	1			1		96.9
BRN2	Nitryl broride: $BrNO_2$			2			1		125.9
BRN3	Bromine nitrate: $BrONO_2$			3			1		141.9
FMBR	Formyl bromide: HC(O)Br	1	1	1			1		108.9
I2	Molecular iodine							2	253.8
I	Iodine atom							1	126.9
IO	Iodine monoxide			1				1	142.9
OIO	Iodine dioxide			2				1	158.9
I2O2	Diiodine dioxide			2				2	285.8
IXOY	Condensable iodine oxides (> I_2O_2)			3				2	301.8
HI	Hydrogen iodide		1					1	127.9
HOI	Hypoiodous acid		1	1				1	143.9
HIO3	Iodic acid: $HONO_2$		1	3				1	175.9
INO2	Nitryl iodide: INO_2			2				1	172.9
INO3	Iodine nitrate: $IONO_2$			3				1	188.9
CH3I	Iodomethane	1	3					1	141.9
MI2	Diiodomethane: CH_2I_2	1	2					2	267.8
MIB	Bromoiodomethane: CH_2BrI	1	2				1	1	220.8
MIC	Chloroiodomethane: CH_2ClI	1	2			1		1	176.4
MBC	Chlorobromomethane: CH_2ClBr	1	2			1	1		129.4
MB2	Dibromomethane: CH_2Br_2	1	2				2		173.8
MBC2	Dichlorobromomethane: $CHCl_2Br$	1	3			2	1		165.8
MB2C	Chlorodibromomethane: $CHClBr_2$	1	3			1	2		210.3
MB3	Bromoform $CHBr_3$	1	1				3		252.7
IALK	Alkyl iodides	3	7					1	170.0
SSCL	Pseudo gas-phase species for sea salt chloride	0				1			35.5
SSBR	Pseudo gas-phase species for sea salt bromide	0					1		79.9
SSN3	Pseudo gas-phase species for sea salt nitrate	0		3	1				62.0

3.0 MODELING DATABASE

We tested and evaluated the halogen chemical mechanism described in Section 2 using the TCEQ's "Rider 8" CAMx model of June 2006. All of the CAMx input data were obtained from the TCEQ with the exception of the oceanic halogen emissions and the boundary conditions for several Br species.

3.1 "Rider 8" Model for June 2006

The TCEQ developed the CAMx "Rider 8" model for use by areas in Texas that are close to the National Ambient Air Quality Standard (NAAQS) for ozone but not designated as nonattainment areas. CAMx input data files were downloaded from: http://www.tceq.texas.gov/airquality/airmod/rider8/rider8Modeling. In summary, meterorological input data were developed using the Weather Research Forecasting (WRF) model and WRFCAMx interface; anthropogenic emissions were based on TCEQ data within Texas and data from EPA outside Texas; biogenic emissions were developed using MEGAN, and; boundary conditions for the outer 36 km grid were extracted from a GEOS-Chem global model simulation of 2006.

The Rider 8 nested modeling grids are shown in Figure 3-1 and the dimensions of grids are given in Table 3-1. The layer structure is defined in Figure 3-2 with 28 layers from the surface to 15 km and a surface layer depth of 34m. The outer 36 km grid covers the continental US (CONUS) and is the same grid that EPA and many States use for regional air quality modeling. The nested 12 km grid covers Texas and a substantial area that would typically be upwind of Texas during an ozone episode including adjacent States and the western Gulf of Mexico. The nested 4 km grid covers the Houston and Dallas ozone nonattainment areas and all of the near nonattainment areas in eastern Texas. CAMx 2-way grid nesting is used to model all grids simultaneously so that pollution transport between grids is modeled without the need for boundary conditions for the nested grids.

Table 3-1. TCEQ 36/12/4 km CAMx nested modeling grids for Rider 8 model of June 2006.

CAMx Grid	Grid Size (number of cells)		
	East-West	North-South	Layers
RPO 36km	148	112	28
Texas 12km	149	110	28
Texas 4km	191	218	28

Figure 3-1. TCEQ 36/12/4 km CAMx nested modeling grids for the Rider 8 model of June 2006. [1]

[1] TCEQ figure from http://www.tceq.texas.gov/airquality/airmod/rider8/modeling/domain.

Vertical Layer Structure

Corresponding WRF Layer	Layer Top (m AGL)	CAMx Layer	Layer Center (m AGL)	Thickness (m)
38	15179.1	28	13637.9	3082.5
36	12096.6	27	10631.6	2930.0
32	9166.6	26	8063.8	2205.7
29	6960.9	25	6398.4	1125.0
27	5835.9	24	5367.0	937.9
25	4898.0	23	4502.2	791.6
23	4106.4	22	3739.9	733.0
21	3373.5	21	3199.9	347.2
20	3026.3	20	2858.3	335.9
19	2690.4	19	2528.3	324.3
18	2366.1	18	2234.7	262.8
17	2103.3	17	1975.2	256.2
16	1847.2	16	1722.2	249.9
15	1597.3	15	1475.3	243.9
14	1353.4	14	1281.6	143.6
13	1209.8	13	1139.0	141.6
12	1068.2	12	998.3	139.7
11	928.5	11	859.5	137.8
10	790.6	10	745.2	90.9
9	699.7	9	654.7	90.1
8	609.7	8	565.0	89.3
7	520.3	7	476.1	88.5
6	431.8	6	387.9	87.8
5	344.0	5	300.5	87.1
4	256.9	4	213.8	86.3
3	170.6	3	127.8	85.6
2	85.0	2	59.4	51.0
1	33.9	1	17.0	33.9

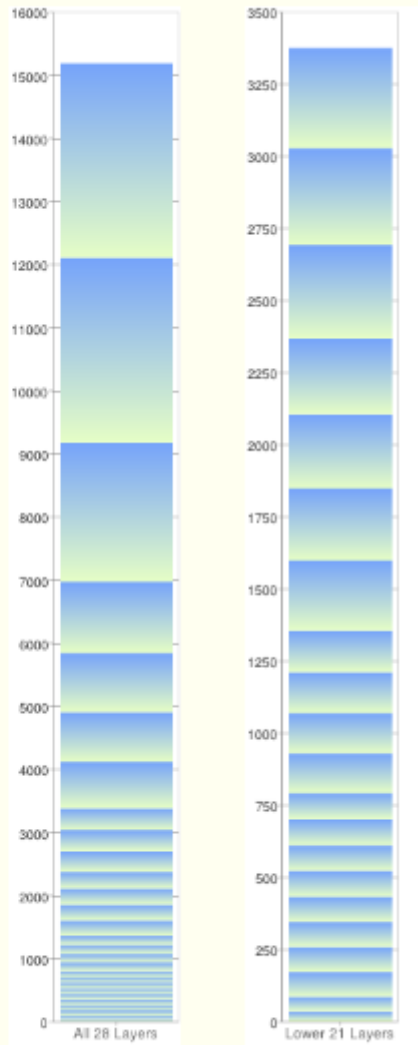

AGL - Above Ground Level.

CAMx vertical layer structure for the Rider 8 model of June 2006. [2]

Figure 3-2. Halogen emissions.

Iodine compounds emitted from ocean waters include molecular iodine (I_2), hypoiodous acid (HOI), methyl iodide (CH_3I), iodochloromethane (CH_2ICl) and diiodomethane (CH_2I_2); bromine compounds emitted include methyl bromide (CH3Br), dibromomethane (CH_2Br_2), bromoform ($CHBr_3$), bromochloromethane (CH_2BrCl), bromoiodomethane (CH_2IBr), bromodichloromethane ($CHBrCl_2$), and dibromochloromethane ($CHBr_2Cl$). Emissions of I_2 and HOI are caused by

[2] TCEQ figure from http://www.tceq.texas.gov/airquality/airmod/rider8/modeling/domain.

deposition of ozone (O_3) to ocean waters (Carpenter et al., 2013; Pillar et al., 2013) whereas emissions of organic iodine and bromine compounds result from biological processes (Carpenter, 2003). Sea-salt aerosol produced by bubble bursting and wind shear at the ocean surface is the dominant source of inorganic Cl and Br input to marine air (Sander et al., 2003). We developed halogen emissions for CAMx as follows.

3.1.1 Halogen emissions from organic sources

Previously, ENVIRON developed a CAMx pre-processor to estimate oceanic emissions of iodine and bromine compounds (Yarwood et al., 2012). Emissions from seawater of halomethanes were estimated from the global emission flux estimates of Ordóñez et al. (2012) allocated spatially and temporally using the seawater content of chlorophyll-a (units of mg/m^3). The SeaWiFS satellite provides chlorophyll-a data with global coverage as monthly averages, as illustrated in Figure 3-3. Global emissions of halomethanes and their spatial distributions are uncertain as discussed recently by Hossaini et al. (2013). The CAMx pre-processor projects the satellite data to a CAMx grid and excludes chlorophyll-a detected in freshwater lakes, as illustrated in Figure 3-4. The halomethane emission factors were calibrated to reproduce global emission budgets (Table 3-2). Emissions of I_2 from seawater were set to a constant emission flux of 4×10^8 molecule cm^{-2} s^{-1} which is between the estimates of Sommariva et al. 2009 (1.2×10^9 molecule cm^{-2} s^{-1} for the remote marine boundary layer) and Mahajan et al. 2010 (5×10^7 molecule cm^{-2} s^{-1}). Emissions of HOI from seawater were not included because quantitative data on emissions are lacking and the emission factor for I_2 likely accounts for iodine input from both I_2 and HOI.

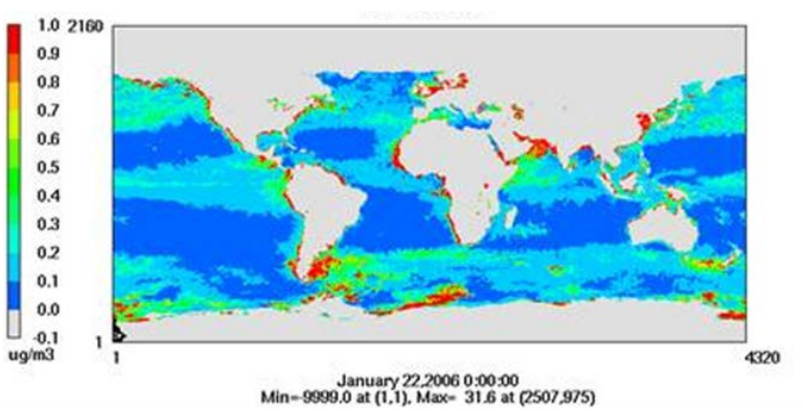

Figure 3-3. Example global sea water concentration of chlorophyll-a (mg/m3) from SeaWiFS satellite data. Note that chlorophyll-a also is detected in freshwater lakes.

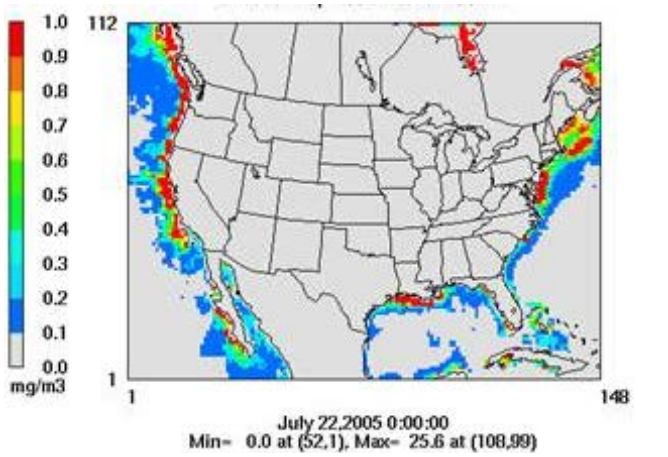

Figure 3-4. Example sea water concentration of chlorophyll-a (mg/m^3) for the CAMx 36 km grid. Note that chlorophyll-a in freshwater lakes has been excluded.

Table 3-2. Global annual emissions of halomethanes.

Compound	Formula	CAMx species name	Global Annual Flux (Gg/year)	Reference
Iodomethane	CH_3I	CH3I	213	Bell et al., 2002
Diiodomethane	CH_2I_2	MI2	116	Ordóñez et al. 2012
Chloroiodomethane	CH_2ICl	MIC	234	Ordóñez et al. 2012
Bromoiodomethane	CH_2IBr	MIB	87.3	Ordóñez et al. 2012
Chlorobromomethane	CH_2BrCl	MBC	10.0	Ordóñez et al. 2012
Dibromomethane	CH_2Br_2	MB2	67.3	Ordóñez et al. 2012
Dichlorobromomethane	$CHBrCl_2$	MBC2	22.6	Ordóñez et al. 2012
Chlorodibromomethane	$CHBr_2Cl$	MB2C	19.7	Ordóñez et al. 2012
Bromoform	$CHBr_3$	MB3	533	Ordóñez et al. 2012

3.1.2 Halogen emissions from sea-salt

Sea-salt aerosols are an important source of halogens in the marine boundary layer (Sander et al., 2003). In the open ocean, marine aerosols are created by turbulence, bubble breaking and viscous shear from winds blowing over the ocean surface. Sea spray particles produced through the action of breaking waves in the surf zone play an important part in processes involving sea salt aerosols in the coastal boundary. Acidification of sea-salt aerosols by nitric (HNO_3) and other acids releases HCl to the atmosphere causing aged sea salt aerosol to be depleted of Cl. Br depletion of sea salt aerosol occurs when HOBr interacts with sea salt aerosol to form Br_2 and this mechanism can occur at neutral as well as acid pH (Yang et al., 2005).

The CAMx sea salt emissions preprocessor can estimate particulate sodium, chloride and sulfate emissions. The sea salt aerosol fluxes from both open oceans and breaking waves in the surf zone are a function of wind speed at 10 meter height. Fluxes are parameterized as a function of wet aerosol radius at a relative humidity of 80%, which is a relative humidity typical of 10 meters elevation in the marine boundary layer. For particles with dry radii more than 4

microns, sea salt particle flux from the open ocean is calculated using the Smith and Harrison (1998) parameterization. For particles with dry radii < 4 microns, either the Gong (2003) or Monahan et al. (1986) parameterization may be used. The surf zone contribution is calculated using the parameterization of DeLeeuw et al. (2000) or the Gong (2003) open ocean parameterization. In this study, the Gong (2003) parameters were used for both open oceans and surf zone.

When CAMx is applied without aerosol species (gas-phase species only) the production of Cl and Br from sea salt is modeled through pseudo gas-phase reactions of species SSCL and SSBR, as discussed above. Emissions of SSCL represent the Cl content of sea salt aerosol in units of moles/hour as required for CAMx gas-phase species. Emissions of SSBR are scaled to SSCL using a molar ratio of 0.00154 based on sea-water compositions (Sander et al., 2003). The scaling of SSBR emissions from SSCL was performed as a post-processing step after running the CAMx sea salt emissions preprocessor to estimate SSCL emissions.

3.1.3 Emission Summary

A summary of halogen emissions for the CAMx 12-km domain is presented in Table 3-3 with daily emissions of CAMx model species in the second column. Emitted halogen species are chemically converted to reactive halogen gases according to their atmospheric lifetimes (third column). Halogens with longer lifetimes (such as MB2 and MB2C) convert slowly and stay longer in the atmosphere (e.g., several months) during which time they can exit the CAMx modeling domain. Instead of analyzing emission contributions based solely on emitted mass, it is more useful to take the atmospheric lifetime in to account. The fraction of emissions that will become available in one day (fourth column) can be calculated from the lifetime by exponential decay. The results show that sea salt aerosol is effectively the only source of Cl (SSCL accounts for 100%) and the dominant source of Br (SSBR accounts for more than 80%). Oceanic I2 is the dominant source of I (i.e.,99%) which is significant because emissions of I2 have greater uncertainty than the emissions of organoiodine compounds.

The spatial distributions of CH_3I, $CHBr_3$, I_2 and SSCL emissions are shown in Figure 3-5 for the 12 km grid on June 17 and 18. The emissions of CH_3I and $CHBr_3$ have the same spatial distribution because they follow that of chlorophyll-a and do not change from June 17 to 18 because the satellite data are chlorophyll-a updated less frequently than daily. I_2 emissions are uniform across ocean grid cells because the emission factor is a constant. Emissions of SSCL are a function of wind speed and so vary in space and time. The SSCL emissions are highest where the sea breeze is strongest on each day.

Table 3-3. Halogen emissions in the CAMx 12 km grid.

CAMx Species Name	Daily[a] Emissions (Tonnes)	Atmos. Lifetime[b] (days)	Fraction Available[d] in 1 day	Emitted Halogen Available Within 1 Day					
				Tonnes			Contribution		
				Cl	Br	I	Cl	Br	I
CH3I	0.9	5	0.18			0.15			0.3%
I2	56.7	0.003	1.00			56.7			98.5%
MB2	0.3	130	0.01		0.0024			0.2%	
MB2C	0.1	145	0.01	0.00012	0.00052		0.000%	0.04%	
MB3	2.0	17	0.06		0.108			7.7%	
MBC2	0.1	46	0.02	0.00061	0.00068		0.000%	0.05%	
MI2	0.5	0.005	1.00			0.47			0.8%
MIB	0.4	0.94	0.65		0.087	0.14		6.2%	0.2%
MIC	1.0	8	0.12	0.024		0.084	0.007%		0.1%
SSBR	2.7	1[c]	0.63		1.20			85.8%	
SSCL	795.3	1[c]	0.63	350.8			100%		
Total				**350.8**	**1.4**	**57.6**	**100%**	**100%**	**100%**

[a] Average of June 17 and 18, 2006
[b] Representative lifetime reported by Ordóñez et al. 2012
[c] Representative lifetime estimated from CAMx results in Chapter 4
[d] Fraction of the halogen precursor that reacts within 1 day based on the atmospheric lifetime

(a) CH_3I

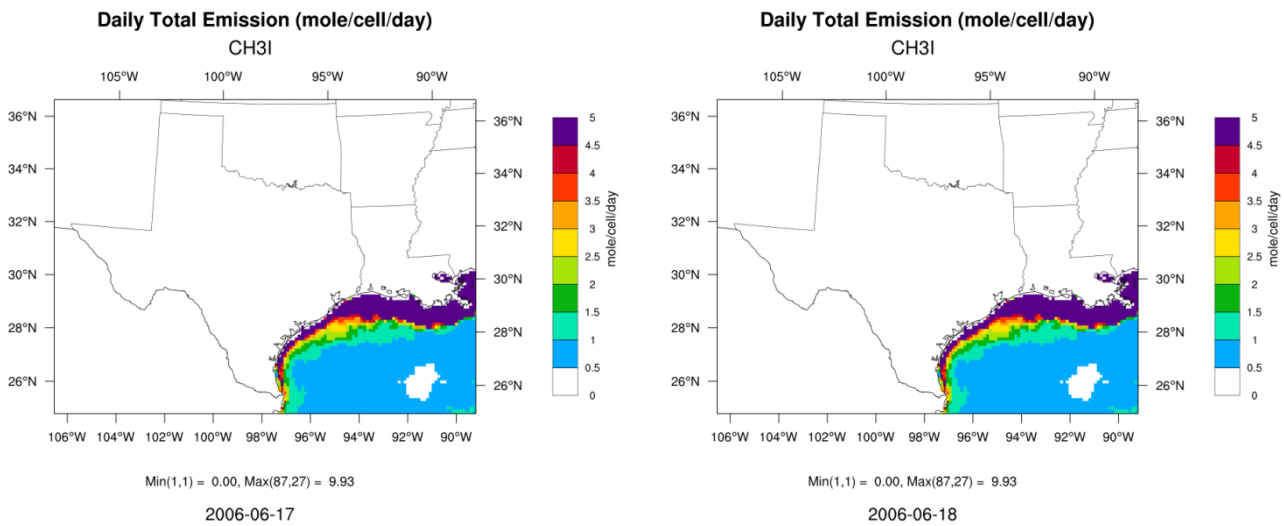

(b) $CHBr_3$

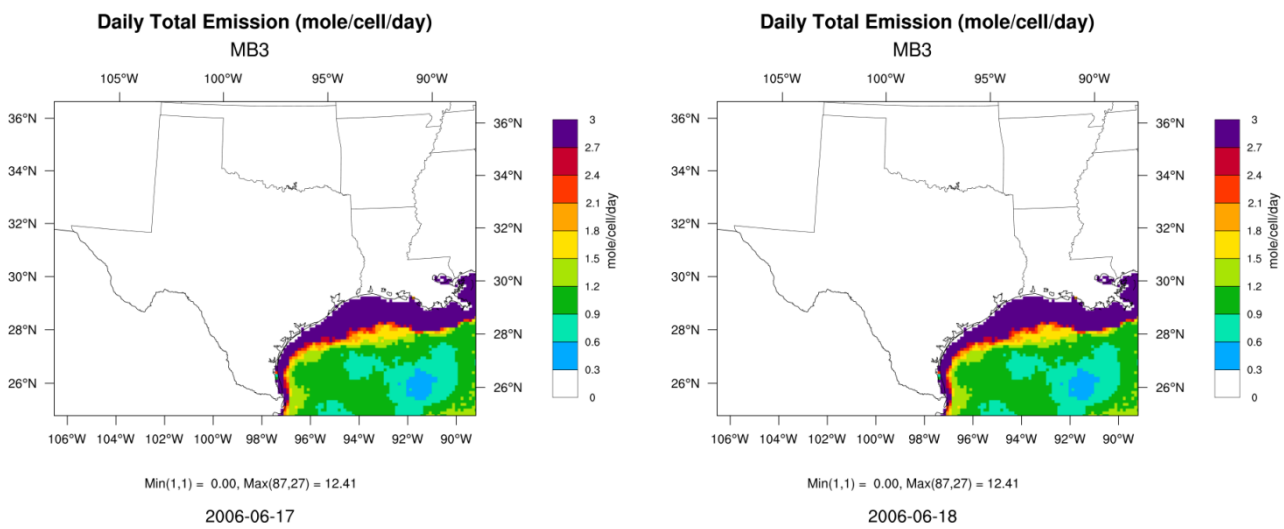

Figure 3-5. Spatial distributions of halogen precursor emissions (moles per grid cell per day) for the 12 km grid on June 17 (left) and June 18 (right) for (a) CH_3I, (b) $CHBR_3$, (c) I_2 and (d) SSCL.

(c) I_2

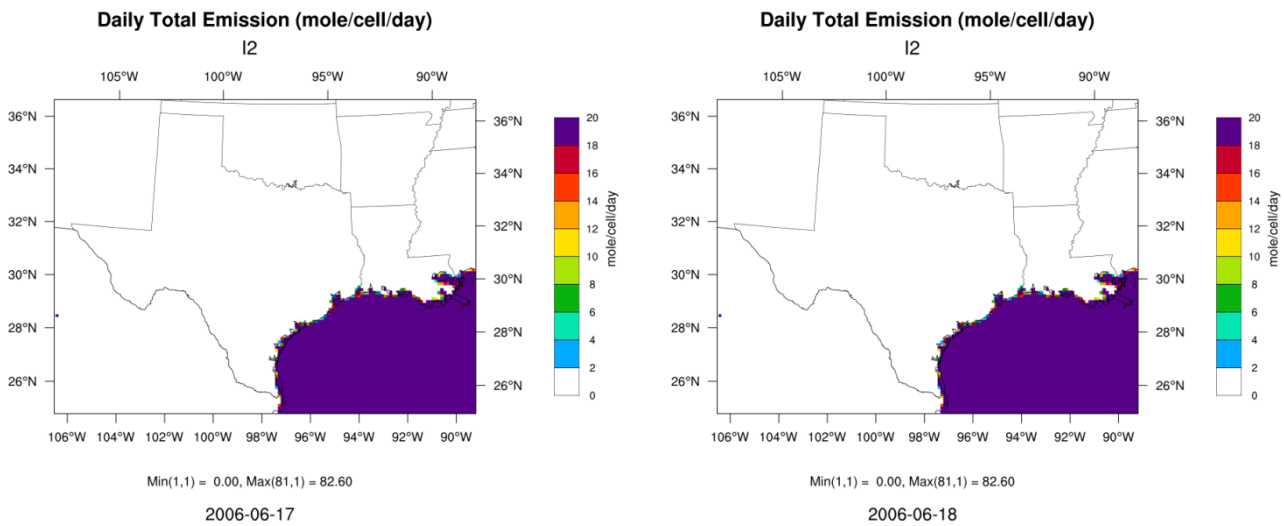

(d) SSCL

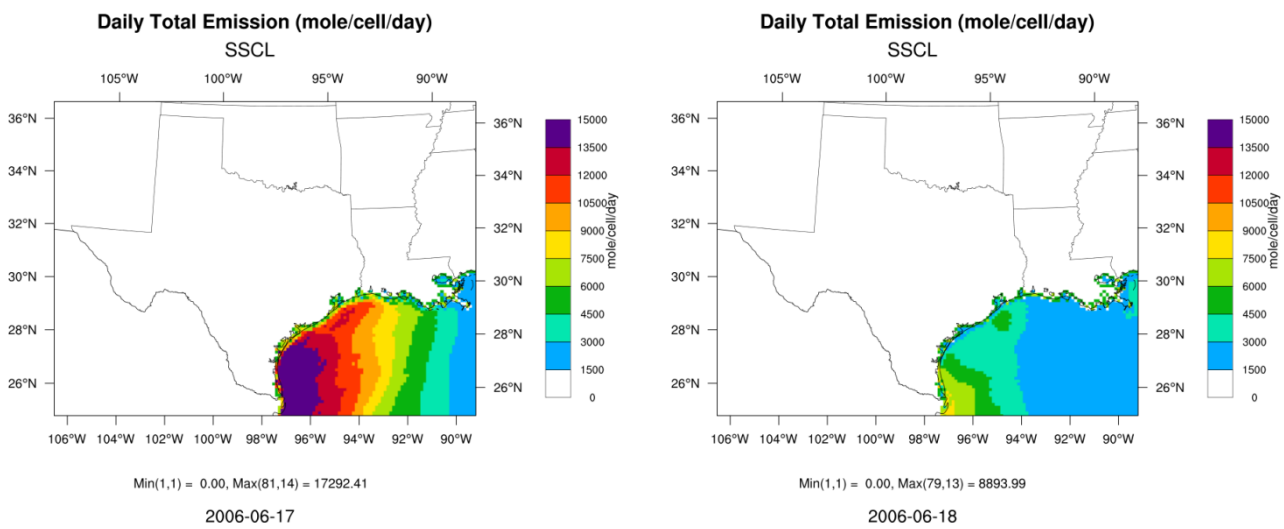

Figure 3-5. (completed) Spatial distributions of halogen precursor emissions (moles per grid cell per day) for the 12 km grid on June 17 (left) and June 18 (right) for (a) CH_3I, (b) $CHBR_3$, (c) I_2 and (d) SSCL.

3.2 Halogen Boundary Conditions

As discussed in Section 3.2.3, several of halomethanes have representative atmospheric lifetimes of several days to months enabling them to be transported into and out of the CAMx 36 km grid. Concentrations of species transported into the 36 km grid are represented by boundary conditions (BCs). A literature review identified representative BCs for CAMx species CH3I, MB3, HBR and HOBR as listed in Table 3-4. The BCs for MB2, MBC, MB2C and MBC2 listed in Table 3-4 were scaled from the MB3 BC according global emissions and atmospheric lifetimes. Specifying a small BC (1 ppt) for HOBR is considered important to initiate activation of sea salt aerosol Br (SSBR) by reaction with HOBr. The species concentrations given in Table 3-4 were added to the CAMx BC files.

Table 3-4. Boundary conditions for halogen species.

CAMx Species	Boundary Condition (ppt)	Reference
CH3I	0.2	Bell et al. (2002)
MB3	0.5	Brinckmann et al. (2012)
MB2	0.8	Scaled from MB3
MBC	0.7	Scaled from MB3
MB2C	0.2	Scaled from MB3
MBC2	0.3	Scaled from MB3
HBR	1.0	Yang et al. (2005)
HOBR	1.0	Yang et al. (2005)

4.0 MODELING RESULTS

The halogen mechanism described in Section 2.2 was integrated with the CB6r2 oxidant mechanism in CAMx version 6.1 and tested using the Rider 8 model developed by TCEQ for June 2006. Oceanic emissions of halogen compounds were estimated using the CAMx emissions pre-processor described in Section 3.2. Analysis of the model results focused on two days with persistent on-shore flow in Texas (June 17 and 18, 2006) when background ozone from the Gulf of Mexico entered Texas (Figure 4-1). Sensitivity tests evaluated differences in ozone due to combined halogen chemistry (i.e., Cl + Br + I) and due to each halogen separately; e.g., the impact of Br alone was determined from a sensitivity test with reaction rates for Cl and I species set to zero.

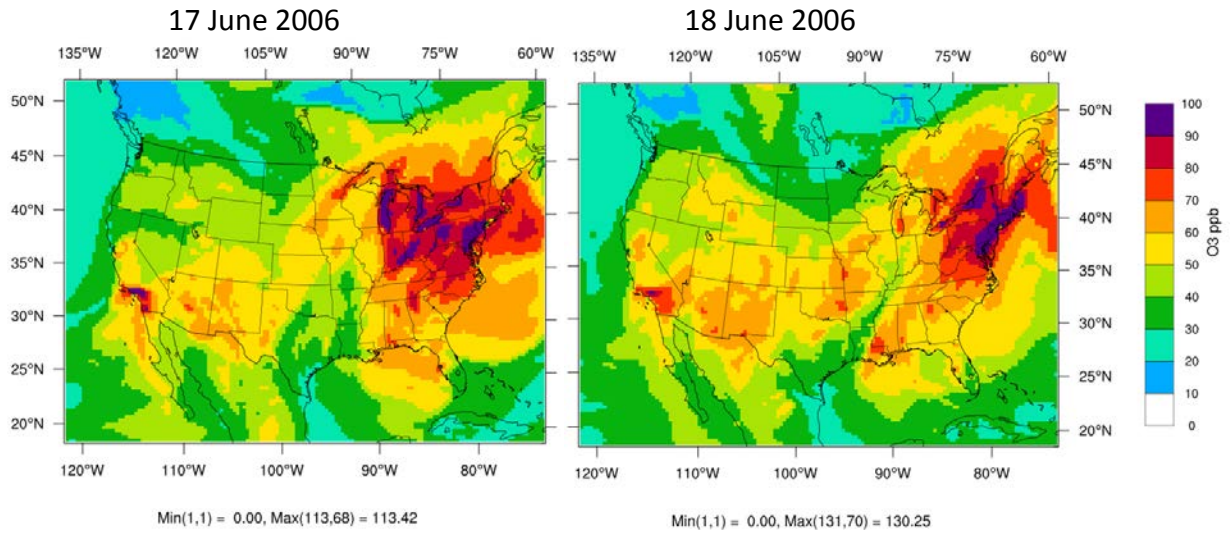

Figure 4-1. MDA8 ozone on June 17 and 18, 2006 (left and right) without halogen chemistry (CB6r2).

Ozone differences due to combined halogen chemistry are shown in Figure 4-2 as changes (reductions) in the daily maximum 8-hour average (MDA8). Halogen chemistry reduces ozone in the Gulf of Mexico, Atlantic Ocean, Pacific Ocean and the Hudson Bay with reductions tending to be larger at lower latitudes where stronger sunlight enhances photochemistry. The largest MDA8 ozone reductions of up to 12 ppb occur in the Pacific Ocean near the Baha peninsula. In the Gulf of Mexico, MDA8 ozone reductions exceed 8 ppb on June 17 and exceed 6 ppb near the Texas coastline on both June 16 and 17. Ozone reductions can be transported onshore and over the CONUS reductions of 2-4 ppb occur in Gulf and Atlantic States from Texas to North Carolina and in Southern California. Onshore ozone reductions are smaller than offshore because the boundary layer deepens and is diluted as air moves onshore and because the halogen emissions considered are from seawater.

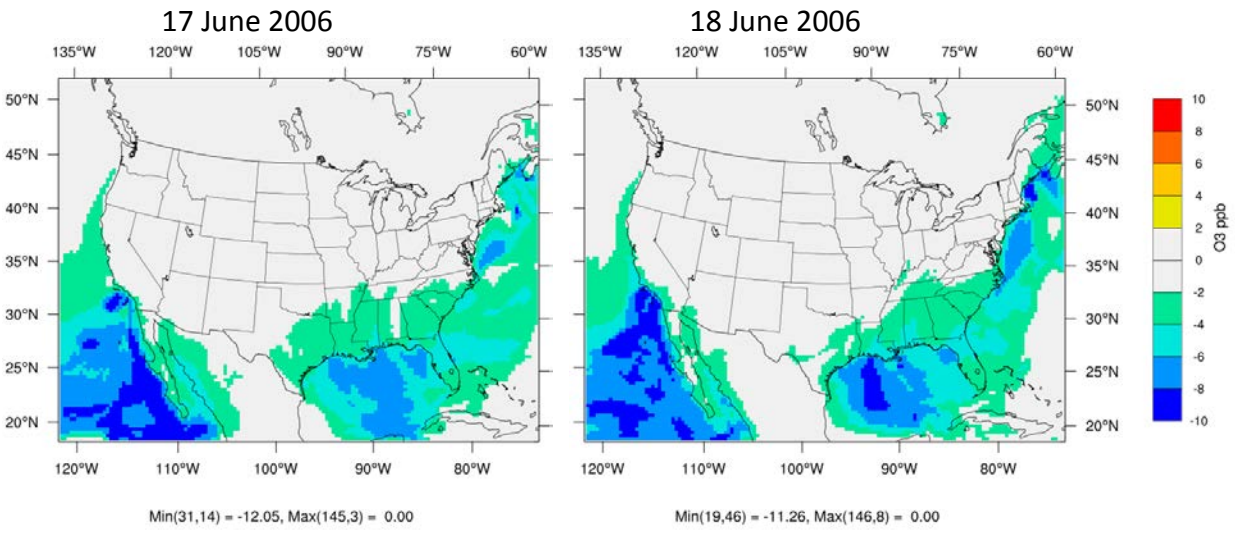

Figure 4-2. Differences in MDA8 ozone on June 17 and 18, 2006 (left and right) due to oceanic emissions and reactions of halogens (CB6r2h – CB6r2).

The contributions of individual halogens to ozone depletion are shown in Figure 4-3 and indicate that Iodine was responsible most of the modeled ozone depletion (this is discussed in more detail below for several locations in Texas). Concentrations of halogen oxides are shown in Figure 4-4 and indicate that iodine and chlorine caused ozone depletion almost exclusively over sea water whereas the influence of Bromine extended inland. This is several of the bromine precursors have atmospheric lifetimes of days or longer (Table 3-3) permitting them to be transported inland and react leading to ozone depletion.

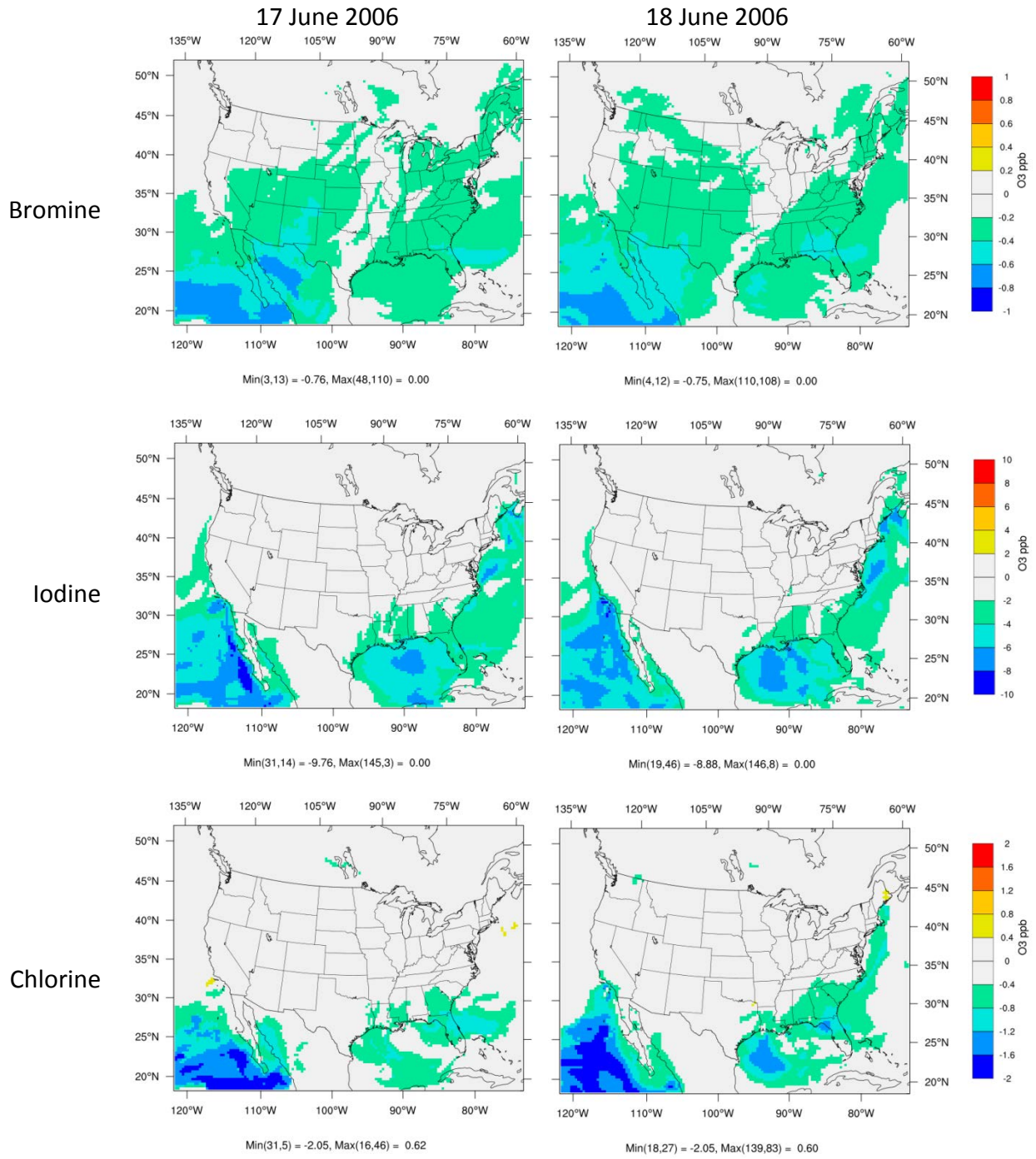

Figure 4-3. Differences in MDA8 ozone on June 17 and 18, 2006 (left and right) due to reactions of Bromine (top), Iodine (middle) and Chlorine (note: scale maxima differ by row).

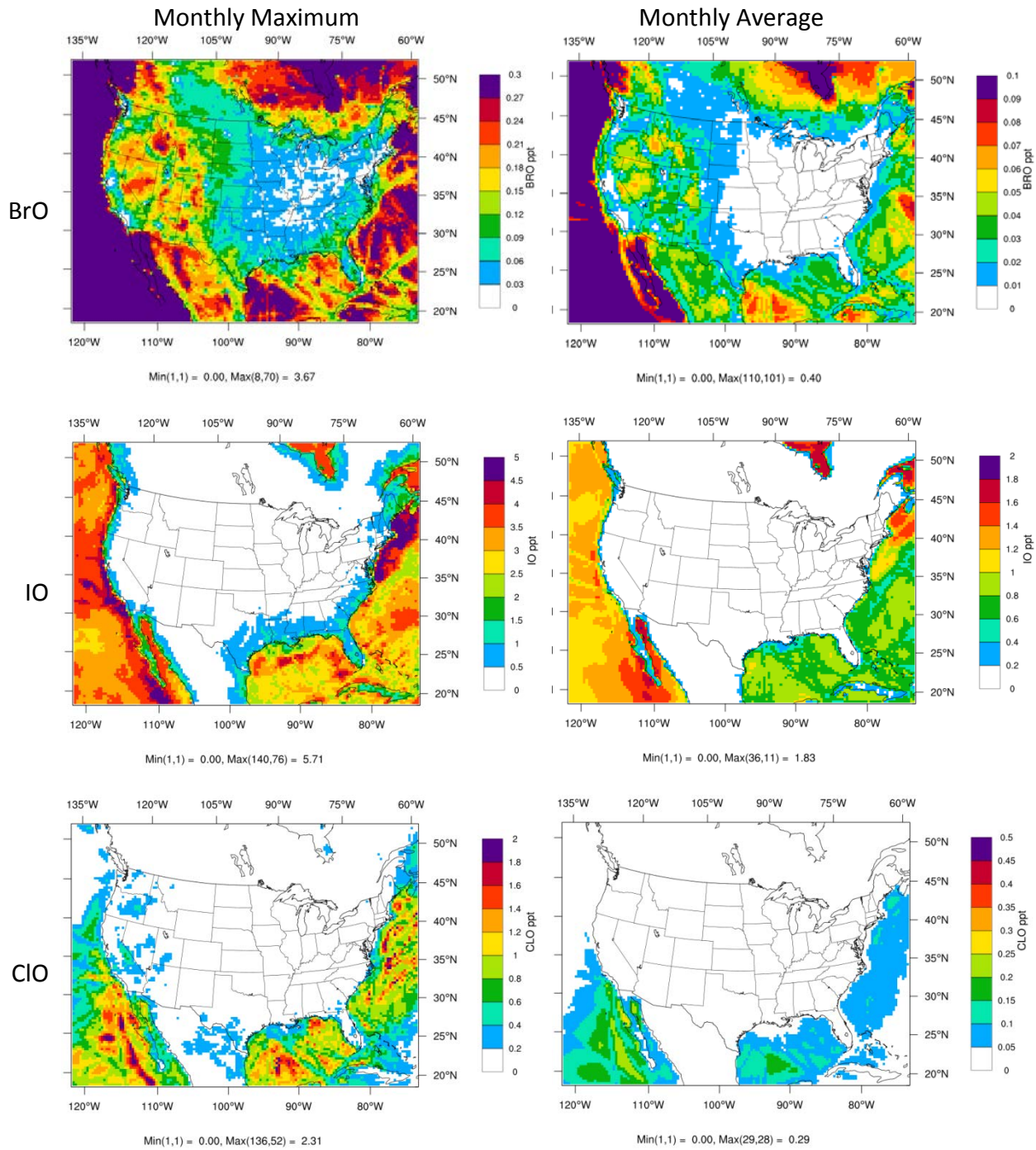

Figure 4-4. Monthly maximum and average (left and right) concentrations of BrO (top), IO (middle) and ClO (note: scale maxima differ by figure).

Further analysis of ozone reductions due to halogen chemistry in Texas considered four receptor locations (where TCEQ collects ozone data at CAMS) near the Gulf Coast, namely:

- Galveston – upwind of Houston when airflow is from the Gulf
- Conroe – downwind of Houston (~120 km from the Gulf) when airflow is from the Gulf
- Sabine Pass – upwind of Beaumont and Port Arthur when airflow is from the Gulf
- Brownsville – near the coastline of the western Gulf, at the Texas-Mexico border.

Hourly profiles of ozone depletion at Galveston and Conroe are shown in Figure 4-5 (June 2006 average) and the contribution of each halogen species to ozone depletion is separated (by sensitivity tests). There is less ozone depletion inland at Conroe than near the coastline at Galveston. Iodine chemistry dominates ozone depletion at both Galveston and Conroe with the same finding at Sabine Pass and Brownsville (Table 4-1). In general, the proportional contributions of I/Br/Cl to ozone depletion at Gulf Coast are approximately 80/10/10.

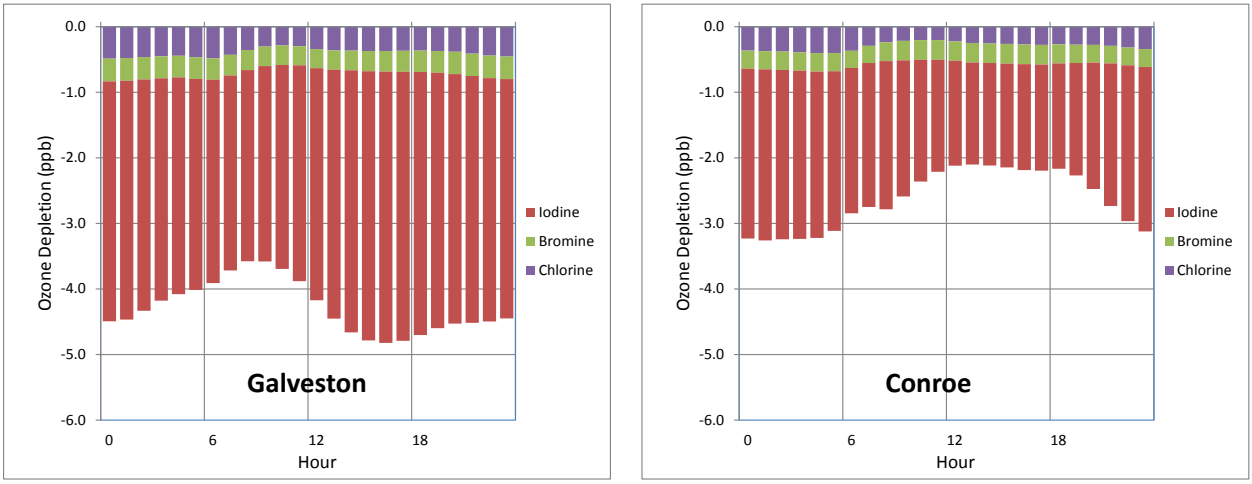

Figure 4-5. Hourly profiles of ozone depletion by halogens at Galveston (left) and Conroe (right) (June 2006 average).

Table 4-1. Daily ozone depletion (ppb) by halogens at Gulf Coast locations (June 2006 average).

Receptor Location	Ozone Depletion (ppb)			Contribution to Ozone Depletion		
	I	Br	Cl	I	Br	Cl
Galveston	-3.57	-0.32	-0.40	83%	8%	9%
Conroe	-2.06	-0.28	-0.30	78%	11%	11%
Sabine Pass	-3.16	-0.30	-0.28	85%	8%	7%
Brownsville	-3.24	-0.33	-0.50	80%	8%	12%

No data are available for Texas to evaluate the magnitude of modeled ozone depletion by halogens summarized in Table 4-1. Measurement data and modeling for the Cape Verde Islands atmospheric observatory (CVAO - in the Atlantic; 17 N, 25 W) find ozone destruction due to I and Br combined of 1.6 ppb/day with I alone contributing 55% of the ozone destruction (Mahajan et al., 2008). Thus, the magnitude of modeled ozone destruction for the Gulf Coast by

I is generally consistent with results from the CVAO but the modeled ozone destruction by Br appears to be too small by roughly a factor of 5.

Halogen monoxide (IO, BrO) concentrations provide a good indicator of ozone destruction because they form when halogen atoms (I, Br) react with ozone. The daytime average IO and BrO from the CVAO are 1.5 and 2.8 ppt, respectively (Mahajan et al., 2008), as compared to modeled daily average IO and BrO for Galveston of 0.47 and 0.014 ppt, respectively (Table 4-2). Thus, IO concentrations are in reasonable agreement (taking into account that a *daytime* average is approximately twice the *daily* average for IO) but the BrO seems low by an order of magnitude. Sea salt is the dominant source of reactive Br (> 80%, Section 3.2.3) and sea salt aerosol at Galveston had modeled Br depletion of 63% indicating that the sea salt Br is being chemically activated to participate in ozone destruction.

Table 4-2. Daily average halogen monoxide (ppt) at receptor locations for June 2006.

Species	Galveston	Conroe	Sabine Pass	Brownsville
ClO	0.025	0.001	0.032	0.017
BrO	0.014	0.004	0.012	0.023
IO	0.47	0.030	0.55	0.15

It appears likely that our CAMx simulations are underestimating reactive Br concentrations and consequently underestimating ozone destruction by Br by a factor of 5 to 10. If this is correct, underestimating the sources of reactive Br appears a more likely explanation than bias in the chemical mechanism because both BrO concentrations and ozone destruction appear similarly underestimated. Sea salt is the dominant source of reactive Br (Section 3.2.3) and evaluating the modeled nitryl chloride concentrations (below) suggests that modeled sea salt concentrations are reasonable. Reasons for the apparent underestimation of reactive Br and consequent ozone destruction are unclear. Measurements of BrO and IO at Galveston would be useful for evaluating models and improving estimates of ozone destruction by halogens in Texas.

Average diurnal concentration profiles for Cl species at Galveston are shown in Figure 4-6 averaged over all days in June 2006. Daily average Cl species concentrations for June 2006 are given in Table 4-3. Three species dominate the diurnal profile: Sea salt chloride (SSCL) peaks in the morning and declines through the day due (in part) to chemical conversion to other species; nitryl chloride forms at night from the reaction of HCl with N_2O_5 on aerosols and decays rapidly by photolysis after sunrise, and; HCl is the main reservoir species (reaction product) for chlorine and is consumed at night by formation of nitryl chloride. Modeled nitryl chloride peaks at 250 ppt before sunrise (251 ppt at 4 am) which is in the middle of the range of nitryl chloride concentrations observed by Osthoff et al. (2008) for the Southeast Texas coastline. Good agreement for nitryl chloride suggests that the sea salt chloride emission estimates and chemistry scheme for nitryl chloride are reasonable. Adding chlorine chemistry and sea salt chloride emissions consistently lowered ozone (Figure 4-5 and Table 4-1) by about 0.5 ppb at the Texas coastline. In contrast, anthropogenic chlorine emissions (of Cl_2 and HOCl) within the

Houston urban area have the potential to increase ozone by tens of ppb (Tanaka et al., 2003b) by accelerating ozone formation in the Houston plume.

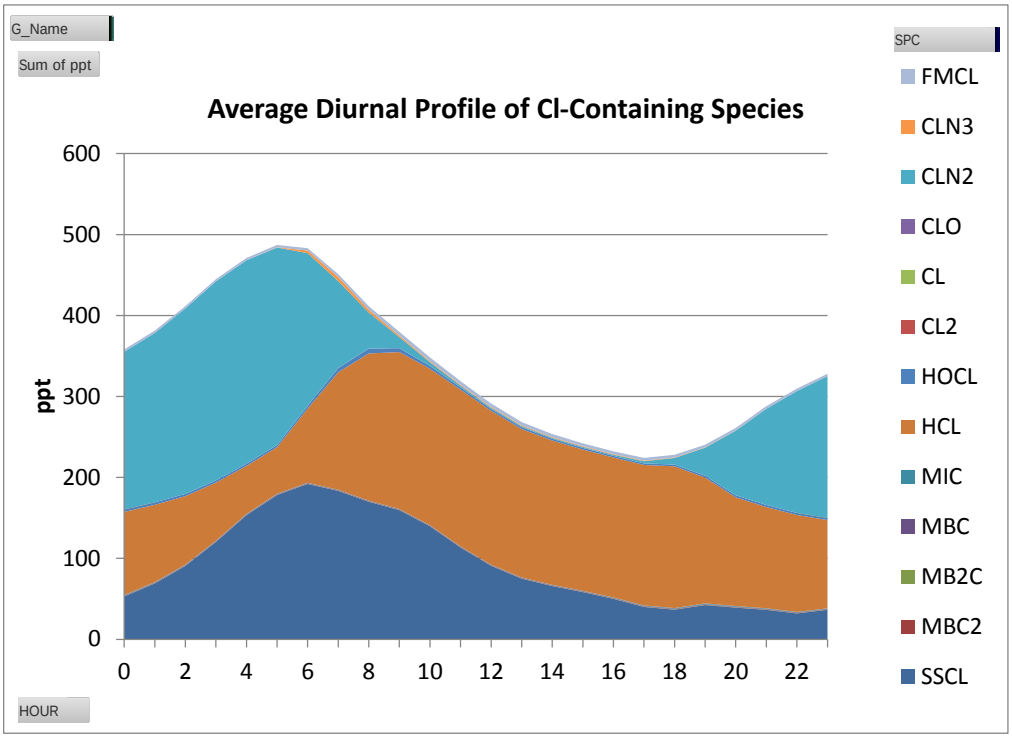

Figure 4-6. Hourly profile of Cl species concentrations (ppt) at Galveston (June 2006 average).

Table 4-3. Daily average halogen species concentrations (ppt) at Galveston (June 2006 average).

Chlorine Species		Bromine Species		Iodine Species	
Halogen precursors (ppt)					
SSCL	92.7	SSBR	0.40	CH3I	0.95
MBC2	0.30	MB3	1.48	MI2	0.070
MB2C	0.23	MB2	0.95	MIC	0.45
MBC	0.68	MB2C	0.23	MIB	0.11
MIC	0.45	MBC	0.68		
		MBC2	0.30		
		MIB	0.11		
Reactive halogens					
CL2	6.20E-07	BR2	0.057	I2	0.53
CL	1.78E-04	BR	9.70E-06	I	0.10
CLO	0.025	BRO	0.014	IO	0.47
				OIO	0.009
HCL	140.07	HBR	0.21	HI	0.034
HOCL	2.92	HOBR	0.61	HOI	4.33
FMCL	3.44	FMBR	8.59E-03		
Nitrogen-containing reactive halogens					
CLN2	96.30	BRN2	5.90E-04	INO2	4.69
CLN3	0.96	BRN3	0.50	INO3	4.84
Higher oxides (aerosol precursors)					
				I2O2	8.01E-05
				IXOY	8.33
				HIO3	2.40

Average diurnal concentration profiles for Br species at Galveston are shown in Figure 4-7 averaged over all days in June 2006. Daily average Br species concentrations for June 2006 are given in Table 4-3. The total concentration of Br precursors (SSBR and halomethanes) exceeds the sum of reactive Br species. Sensitivity test results confirmed that Br precursors are being consumed by chemical reactions releasing reactive Br as shown in Table 4-4. The more reactive species (SSBR and MIB) are most depleted (> 62%) and the less reactive species (MBC, MB2, MB2C, MBC2) are least depleted (< 15%). MIB reacts more rapidly than other Br-containing halomethanes because the presence of a C-I bond in MIB greatly increases the photolysis rate. The main reservoir species for reactive Br are $BrNO_3$ during the day, HOBr at night and HBr throughout the day. Some Br_2 accumulates at night and is formed by the reaction of HOBr with sea salt (SSBR) but Br_2photolyzes rapidly after sunrise. Very little nitryl bromide ($BrNO_2$) accumulates, in contrast to nitryl chloride, and the species BRN2 could be eliminated from the Br mechanism.

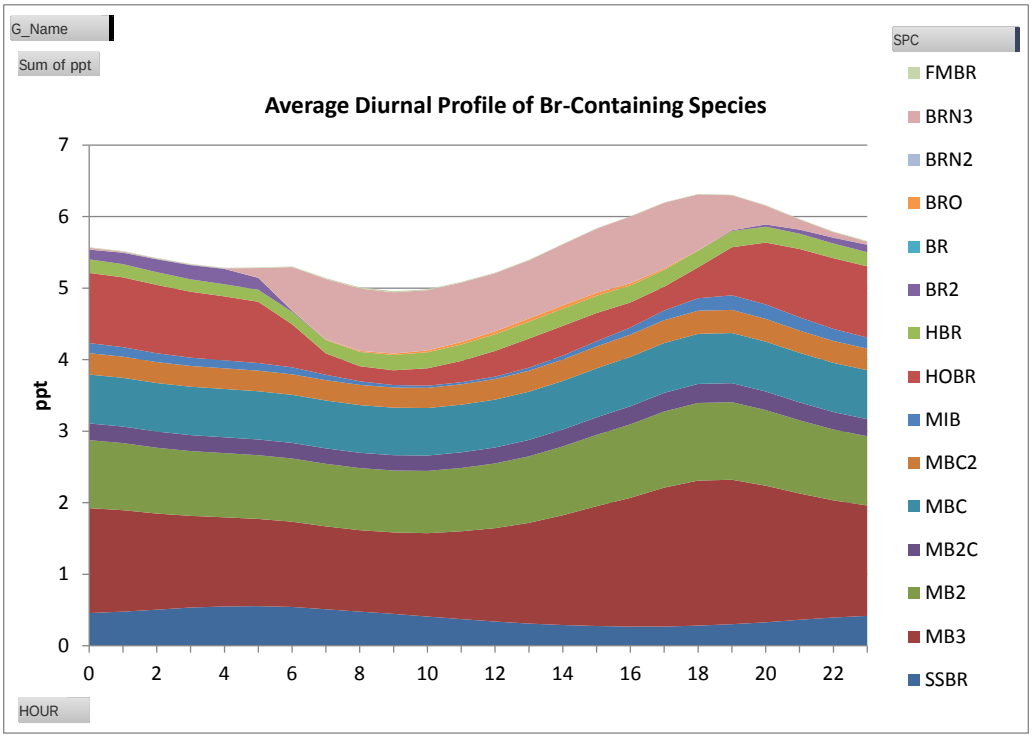

Figure 4-7. Hourly profile of Br species concentrations (ppt) at Galveston (June 2006 average).

Table 4-4. Chemical destruction of Br precursors at Galveston (June 2006 average).

CAMx Species	Description	Depletion
SSBR	Sea Salt Bromide	63%
MB3	$CHBr_3$	19%
MB2	CH_2Br_2	13%
MB2C	CH_2Br_2Cl	14%
MBC	CH_2BrCl	4%
MBC2	$CHBrCl_2$	15%
MIB	CH_2IBr	62%

Average diurnal profiles of I species concentrations at Galveston are shown in Figure 4-8 averaged over all days in June 2006. Daily average I species concentrations for June 2006 are given in Table 4-3. The total concentration of reactive I species exceeds that of I precursors (CH_3I, MI2, MIB, MIC and I_2), in contrast to Br, because I precursors react rapidly by photolysis. The main reservoir species for reactive I in the gas phase are INO_3 during the day and HOI at night. Some I_2 is apparent at night due to direct emissions from seawater but I_2 photolyzes rapidly during the day and provides the dominant source of I (Section 3.2.3). The aerosol forming species IXOY and HIO_3 accumulate a substantial fraction of total I and are the main sink for reactive I that limits ozone destruction.

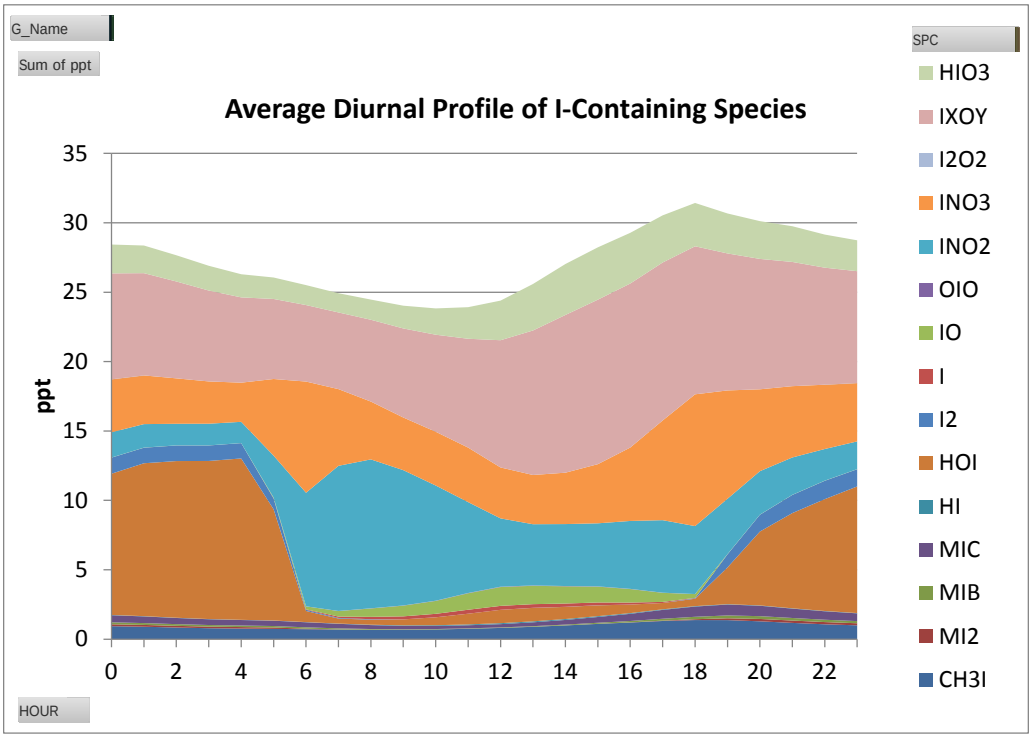

Figure 4-8. Hourly profile of I species concentrations (ppt) at Galveston (June 2006 average).

5.0 CONCLUSIONS AND RECOMMENDATIONS

We developed a chemical mechanism for halogens (Cl, Br and I) that is compatible with the latest version of the Carbon Bond chemical mechanism implemented in CAMx, namely revision 2 of Carbon Bond 6 (CB6r2). The halogen mechanism has 86 reactions and 41 species in addition to the 216 chemical reactions and 80 chemical species of CB6r2. When these halogen reactions are combined with CB6r2 the mechanism may be referred to as CB6r2h. CAMx simulations times with CB6r2h are about double those for CB6r2 when aerosols are not modeled explicitly.

We developed a CAMx pre-processor to estimate emissions of halogen precursors from sea water, namely sea salt, molecular iodine and 9 halomethanes. Halomethane emissions are estimated using the method of Ordóñez et al. (2012) whereby emission rates are proportional to the water content of chlorophyll-a which is available with global coverage as monthly averages measured by the SeaWiFS satellite.

Halogen chemistry reduces ozone in the Gulf of Mexico, Atlantic Ocean, Pacific Ocean and the Hudson Bay with reductions tending to be larger at lower latitudes where stronger sunlight enhances photochemistry. In the Gulf of Mexico, MDA8 ozone reductions exceeded 6 ppb near the Texas coastline. Ozone reductions can be transported onshore and over the CONUS reductions of 2-4 ppb occurred in Gulf and Atlantic States from Texas to North Carolina. Onshore ozone reductions are smaller than offshore because the boundary layer deepens and is diluted as air moves onshore and because the halogen emissions considered are from seawater.

No data are available for Texas to evaluate the magnitude of modeled ozone depletion by halogens. Measurement data and modeling for the Cape Verde Islands (in the Atlantic; 17 N, 25 W) find ozone destruction due to I and Br combined of 1.6 ppb/day with I alone contributing 55% of the ozone destruction (Mahajan et al., 2008). Thus, the magnitude of modeled ozone destruction for the Gulf Coast by I is generally consistent with results from the Cape Verde Islands but the modeled ozone destruction by Br appears to be too small by roughly a factor of 5.

Adding Cl chemistry and sea salt chloride emissions consistently lowered ozone by about 0.5 ppb at the Texas coastline. In contrast, anthropogenic chlorine emissions within the Houston urban area have the potential to increase ozone by tens of ppb (Tanaka et al., 2003b) by accelerating ozone formation in the Houston plume.

It appears likely that our CAMx simulations under estimated reactive Br concentrations and consequently under estimated ozone destruction by Br by a factor of 5 to 10. If this is correct, underestimating the sources of reactive Br appears a more likely explanation than bias in the chemical mechanism because both BrO concentrations and ozone destruction appear similarly under estimated. However, reasons for the apparent underestimation of reactive Br and consequent ozone destruction are unclear. Measurements of BrO and IO at Galveston would be useful for evaluating models and improving estimates of ozone destruction by halogens in Texas. The halogen mechanism and this modeling should be reviewed and updated when new

data become available, such as measurements of BrO and IO in Texas. Modeling model sea salt aerosol explicitly would allow sea salt aerosol concentrations to be evaluated.

6.0 REFERENCES

Bell, N., L. Hsu, D. J. Jacob, M. G. Schultz, D. R. Blake, J. H. Butler, D. B. King, J. M. Lobert, and E. Maier-Reimer (2002). "Methyl iodide: Atmospheric budget and use as a tracer of marine convection in global models. " *Journal of Geophysical Research: Atmospheres* 107, no. D17: ACH-8.

Brinckmann, S., A. Engel, H. Bönisch, B. Quack, and E. Atlas (2012). "Short-lived brominated hydrocarbons–observations in the source regions and the tropical tropopause layer." *Atmospheric Chemistry and Physics* 12, no. 3: 1213-1228.

Carpenter, L. J., S. M. MacDonald, M. D. Shaw, R. Kumar, R. W. Saunders, R. Parthipan, J. Wilson, and J. M.C. Plane (2013). "Atmospheric iodine levels influenced by sea surface emissions of inorganic iodine." Nature Geoscience 6, no. 2: 108-111.

Carpenter, L.J. 2003. Iodine in the marine boundary layer. Chemical Reviews 103, 4953-4962.

ENVIRON (2014) User's Guide to CAMx version 6.10, available at http://www.camx.com/

IUPAC Subcommittee for Gas Kinetic Data Evaluation (2014a). "Summary of Reactions and Preferred Rate Data, Volume 3 - Inorganic Halogen Species." Available at http://iupac.pole-ether.fr/datasheets/summary/vol3_summary.xml.

IUPAC Subcommittee for Gas Kinetic Data Evaluation (2014b). "Summary of Reactions and Preferred Rate Data, Volume - Organic Halogen Species." Available at http://iupac.pole-ether.fr/datasheets/summary/vol4_summary.xml.

Hossaini, R., Mantle, H., Chipperfield, M. P., Montzka, S. A., Hamer, P., Ziska, et al. (2013). "Evaluating global emission inventories of biogenic bromocarbons." *Atmospheric Chemistry and Physics*, *13*(23), 11819-11838.

Koo, B., G. Yarwood and J. Roberts (2012). "An Assessment of Nitryl Chloride Formation Chemistry and its Importance in Ozone Non-Attainment Areas in Texas." Final report for Texas Air Quality Research Program project 10-015, available at http://aqrp.ceer.utexas.edu/projectinfo%5C10-015%5C10-015%20Final%20Report.pdf.

Mahajan, A. S., J. M. C. Plane, H. Oetjen, L. Mendes, R. W. Saunders, A. Saiz-Lopez, C. E. Jones, L. J. Carpenter, and G. B. McFiggans (2010). "Measurement and modelling of tropospheric reactive halogen species over the tropical Atlantic Ocean." *Atmos. Chem. Phys.*, 10, 4611-4624, 2010 doi:10.5194/acp-10-4611-2010

Osthoff, H. D., J. M. Roberts, A. R. Ravishankara, E. J. Williams, B. M. Lerner, R. Sommariva, and S. S. Brown (2008). "High levels of nitryl chloride in the polluted subtropical marine boundary layer." *Nature Geoscience*, 1(5), 324-328.

Ordóñez, C., J.-F. Lamarque, S. Tilmes, D.E. Kinnison, E.L. Atlas, D.R. Blake, G. Sousa Santos, G. Brasseur, and A. Saiz-Lopez (2012) "Bromine and iodine chemistry in a global chemistry climate model: description and evaluation of very short-lived oceanic sources," *Atmos. Chem. Phys.*, 12, 1423-1447, doi:10.5194/acp-12-1423-2012.

Parrella, J. P., D.J. Jacob, Q. Liang, Y. Zhang, L. J. Mickley, B. Miller, M. J. Evans et al. (2012) "Tropospheric bromine chemistry: implications for present and pre-industrial ozone and mercury." *Atmospheric Chemistry and Physics* 12, no. 15: 6723-6740.

Pillar, E.A., M.I. Guzman, and J.M. Rodriguez (2013). "Conversion of Iodide to Hypoiodous Acid and Iodine in Aqueous Microdroplets Exposed to Ozone." *Environmental Science & Technology* 47.19: 10971-10979.

Smoydzin, L., and R. von Glasow (2012). "Modelling chemistry over the Dead Sea: bromine and ozone chemistry." *Atmospheric Chemistry and Physics* 9, no. 14: 5057-5072.

Tanaka, P.L., D. T. Allen, E. C. McDonald-Buller, S. Chang, Y. Kimura, C.B.Mullins, G. Yarwood, and J.D. Neece (2003a). "Development of a chlorine mechanism for use in the carbon bond IV chemistry model." *Journal of Geophysical Research: Atmospheres,* 108(D4), 1984–2012.

Tanaka, P. L., Riemer, D. D., Chang, S., Yarwood, G., McDonald-Buller, E. C., Apel, E. C., ... & Allen, D. T. (2003b). "Direct evidence for chlorine-enhanced urban ozone formation in Houston, Texas." *Atmospheric Environment*, 37(9), 1393-1400.

Whitten, G. Z., and G. Yarwood (2008). "The Ozone Productivity of n-Propyl Bromide: Part 2—An Exception to the Maximum Incremental Reactivity Scale." *Journal of the Air & Waste Management Association* 58, no. 7: 891-901.

Vogt, R., R. Sander, R. von Glasow, and P.J. Crutzen (1999). "Iodine chemistry and its role in halogen activation and ozone loss in the marine boundary layer: A model study." *Journal of Atmospheric Chemistry* 32, no. 3: 375-395.

Yang, X., R.A. Cox, N.J. Warwick, J.A. Pyle, G.D. Carver, F.M. O'Connor, and N.H. Savage (2005). "Tropospheric bromine chemistry and its impacts on ozone: A model study." *Journal of Geophysical Research: Atmospheres* 110, no. D23.

Yarwood, G., J. Jung, U. Nopmongcol and C. Emery (2012). Improving CAMx Performance in Simulating Ozone Transport from the Gulf of Mexico, Final Report for Work Order No. 582-11-10365-FY12-05.